UNITED STATES DEPARTMENT OF THE INTERIOR
GEOLOGICAL SURVEY

A FIELD STUDY OF LITTORAL PROCESSES IN ESTERO BAY, CALIFORNIA

by

John R. Dingler, Roberto J. Anima, David E. Molzan,
Gretchen Luepke, and Curt L. Peterson

Open-File Report 82-537

This report is preliminary and
has not been reviewed for
conformity with U.S. Geological
Survey editorial standards.

Menlo Park, California
June, 1982

A FIELD STUDY OF LITTORAL PROCESSES IN ESTERO BAY, CALIFORNIA

by

John R. Dingler, Roberto J. Anima, David E. Molzan,
Gretchen Luepke, and Curt L. Peterson

ABSTRACT

Estero Bay, which lies on the central California coast, has rocky headlands at both ends and sandy beaches within it. The shoreline of the bay has adjusted to be in equilibrium with the predominant wave climate, which is from the northwest. Because of its present shoreline configeration, the net southward littoral transport found along much of the California coast does not occur within Estero Bay. Instead, the sand primarily moves on- and offshore with a reversing longshore component. This sand transport pattern produces a littoral cell within Estero Bay even though there is no submarine canyon in the area. The primary sand sinks for this cell appear to be the sand spit south of Morro Rock and the entrance to Morro Bay itself, although this opinion was not experimentally verified.

Field work during one summer (1978) and the following winter (1979) produced baseline data on the profile of and grain-size distribution across the littoral zone. In the offshore part of the littoral zone we also studied ripple size and type, internal structure, depth of erosion, and mineralogy. Although these data, which were collected along nine transects spaced 2 km apart, are inadequate to yield transport and energy rates, they indicate a northward decrease in wave energy within Estero Bay and a mixing of the sediments in the offshore. Box core and rod height data from grid points in seven meters of water showed that on the order of a meter of erosion occurred in the central part of the bay between the two sampling periods. Offshore, the data were incomplete, but at one station, in 17 m of water, at least 20 cm of erosion occurred.

INTRODUCTION

Between Point Conception and Point Sur, the central California coast contains two named and several unnamed crenulate-shaped bays. All of these bays have the same orientation; their curved section of coastline is north of the tangential section. The four largest of these bays occur in close proximity to each other between Point Arguello and Point Estero. Each is separated from the next by a prominent rocky headland, and they all have sandy beaches within them. Estero Bay, the northmost of the four bays, is unique because its coastline is broken in the middle by a large dacite plug (Morro Rock). It also is the only one of the four bays to contain a large lagoon (Morro Bay), even though both San Luis Obispo Bay and the unnamed bay between Point Arguello and Purisima Point have larger rivers entering them. In terms of beach size, both Estero Bay and San Luis Obispo Bay have long, wide beaches, which have built onto old flood plains. In the other two bays, the beaches are more confined both in length and width. Figure 1 locates the major coastal features just described; it also shows the submarine canyons occurring off this section of coastline.

Silvester (1974) studied crenulate-shaped bays in both the laboratory and the field. From his model studies, he concluded that the crenulate-shape is the equilibrium one for bays on coasts where there is a dominant, oblique direction from which swell waves approach. In essence, the sandy coast between rocky headlands adjusts so that it is parallel to the refracting and defracting waves from the dominant direction. This means that extensive erosion occurs at the upwave end of the bay, causing that area to become very curved. Sediment transport is in the downwave direction where defraction is absent and refraction is less extensive; consequently, the downwave end of the bay ends up fairly straight with sand building out toward the seaward edge of the headland (see Silvester, 1974, p. 73). When the coastline within a bay parallels the breaking waves, longshore transport ceases; waves approaching from another direction will disrupt this equilibrium and reinitiate sediment transport in the downwave direction.

Swell waves predominantly approach the central California coast from the northwest (Gerdes, et al, 1974, p. 17) so orientation of the crenulate-shaped bays is consistent with Silvester's hypothesis. Net sand transport, which is expected to be in the same direction as the net longshore component of wave energy, should be towards the south along the central California coast. This has been quantified by Bowen and Inman (1966) for the coast south of Pismo Beach. The net sand transport direction from Estero Bay to Pismo Beach has not been verified, although there are indications that it is not generally to the south. Based on the abundance of the heavy mineral augite along the central California coast, Trask (1952) concluded that some sand from Estero Bay or northern San Luis Obispo Bay reached Santa Barbara. Bowen and Inman stated that little sediment entered the north end of San Luis Obispo Bay around Point Buchon. Shepard and Wanless (1971, p. 311) stated that a counter-current exists in the southern half of Estero Bay that produces northward littoral sand transport. Noda and Jen (1975) also concluded that sand moved northward along the long spit south of Morro Rock, based on hindcasting and spit shape. The Corps of Engineers (Gerdes, et al, 1974, p. 33) dredges the Morro Bay entrance channel every few years; the most reasonable supply of that sand is the spit.

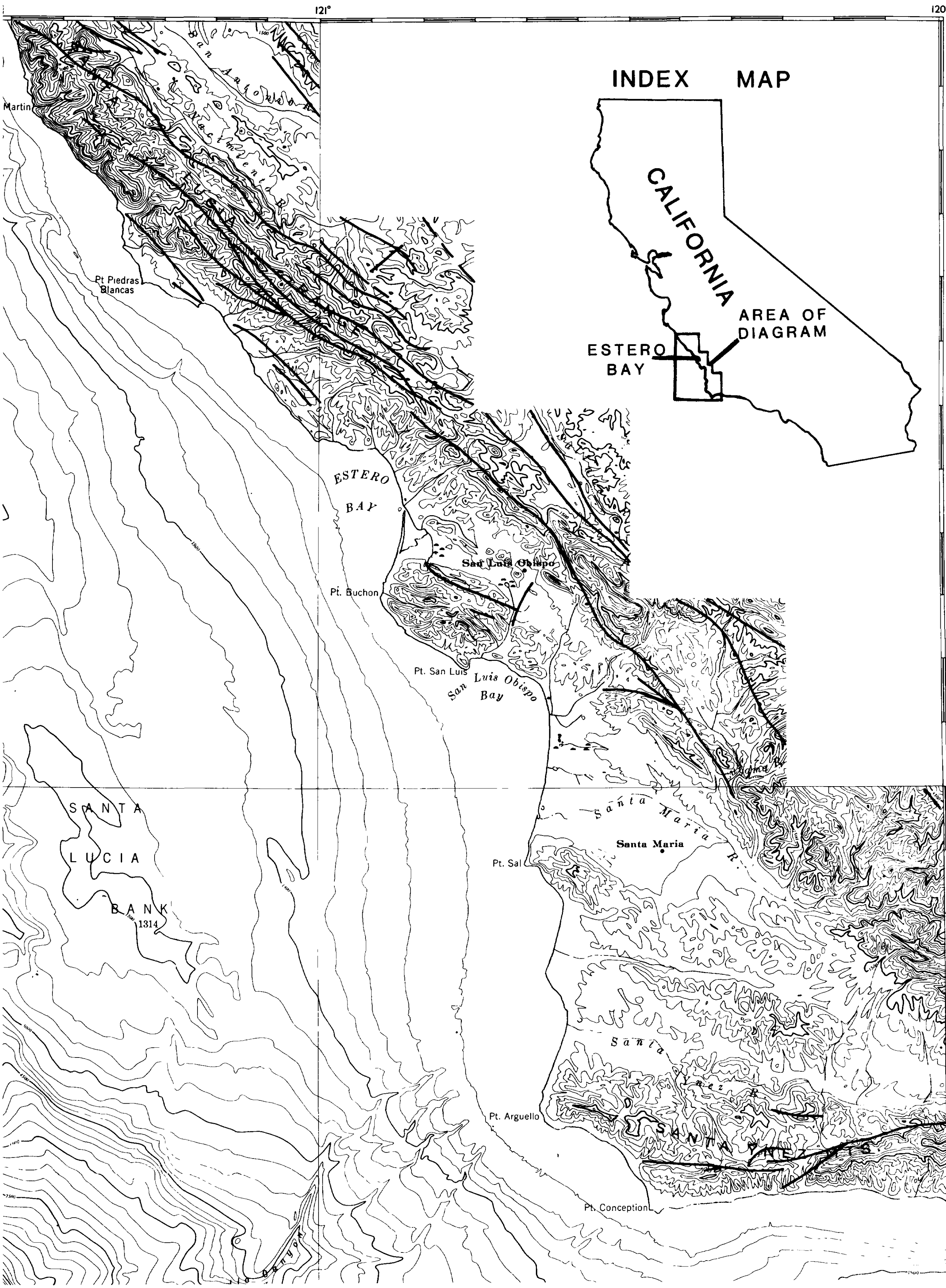

Figure 1. Location map for the central California coast, including major offshore features (adapted from Shepard and Emery, 1941).

Inman and Frautschy (1966) divided the southern California coastal region into discreet sedimentation units, called littoral cells. Each cell contains a complete cycle of sedimentation from sources, which supply sand to the cell; through littoral transport, which moves the sand along the coast; to sinks, which permanently remove the sand from the littoral zone. The littoral zone comprises the beach and the wave-dominated coastal waters; along the Pacific Coast, it typically extends from the seaward limit of vegetation or cliffs to a depth of around twenty meters. The primary sand sources along the California coast are rivers and coastal cliffs; the primary sinks are submarine canyons and coastal sand dunes.

Characteristically, a southern California littoral cell has a rocky headland at its updrift end and a submarine canyon at its downdrift end. In between, beaches exist that receive sand from sources and from littoral drift. Sand movement in the littoral zone is often interrupted by storms, which carry some of the sand offshore from where swell slowly moves it back to the beach face.

Estero Bay does not have a submarine canyon at either end; however, if not very much sand moves around the headlands, then Estero Bay should be considered a littoral cell. In this case, instead of having a submarine canyon as a major sink, sand would circle throughout the bay with predominantly on- and offshore movement, supplemented by littoral transport in first one direction and then the other. Such a situation is reasonable if sand sources are minor, and if the shoreline configuration is essentially in equilibrium with the wave climate. The latter factor is essential to this concept because it means that littoral transport is small, and no net transport exists in a southerly direction. Sand would only be lost from the cell when it moves onto the spit, into deep water, or into Morro Bay.

Several investigators have discussed foreshore slopes (see Komar, 1976, p. 303), and they concluded that slope is controlled by two factors: grain size and wave energy. Bascom (1951), after profiling many west coast, high-energy beaches, concluded that beach slopes and grain sizes could be compared across time and distance and between investigators. To accomplish such comparisons, each investigator had to measure beach slope and grain-size at a "reference point." Bascom described the reference point as that part of the beach face subject to wave action at mid-tide elevation. Samples taken above or below the reference point tended to deviate in non-systematic ways; the largest deviations were associated with the coarsest beaches. Bascom presented his data in a plot of beach-face slope versus grain size; Wiegel (1964) added data from east coast low-energy beaches to Bascom's plot. The resulting plot (see for example, Fig.10) shows that beach face slope increases with grain size, and that low-energy beaches are steeper than high-energy ones of comparable sand.

Bascom noted that a beach can change latterly from a low-energy shape to a high-energy one; he used Half Moon Bay, California as an example. The trend at Half Moon Bay is from a low-energy slope at the protected, north end of the beach to a high-energy slope at the south end.

Little published data exists on sedimentary processes within Estero Bay. In addition to the Noda report, information on coastal sediments and/or processes are restricted to generalized statements (e.g., BLM, 1980; Standard Oil Company, 1974) or to remarks in papers of wide areal scope (e.g., Trask, 1952; Bascom, 1951; Cooper, 1967). The onshore and offshore geologic studies that exist (e.g., Chipping, 1979; Hall, 1975) apply to the coastal zone only in an indirect way.

This report presents the initial phase of a study of coastal sediments and processes within Estero Bay. It deals in varying degrees with the general profile, distribution of sediments and bedforms, seasonal changes, and mineralogy. As such, it provides baseline data on these items as well as general interpretations of sediment movement and wave energy within the bay.

LOCATION

Estero Bay indents the California coast midway between Los Angeles and San Francisco. Between its bounding rocky headlands, Point Buchon to the south and Point Estero to the north, the shore of the bay primarily consists of sandy beaches. Morro Rock, an Oligocene dacite plug (Hall, 1973), crops out in the littoral zone in the center of the bay. North of Morro Rock, small rocky outcrops divide the sharply curving coast into several, short beaches that are generally narrow and are backed by low-lying bluffs of Franciscan material (Hall and Pryor, 1975). The only exception is the beach adjacent to Morro Rock, which is backed by low-lying sand dunes. Several of these beaches receive sediment directly from small, ephemeral streams; the total watershed north of Morro Bay is 185 km^2.

From Morro Rock south to Hazard Canyon, the beach is continuous and gently curving. For most of this distance the beach is part of a barrier spit that is covered with large sand dunes; in the vicinity of Hazard Canyon, the beach abutts bluffs of the Pismo Formation (Hall, 1973). The coast is unbroken by streams and outcrops between the entrance to Morro Bay and Hazard Canyon; from there south to Point Buchon, rocks crop out and two small creeks, draining 47 km^2, enter the littoral zone.

The spit separates Estero Bay from Morro Bay, a large lagoon that includes approximately 10 km^2 of water surface and salt marsh at high tide (Gerdes, et al, 1974, p. 19). The entrance to Morro Bay is on the south side of Morro Rock, although, at one time entrances existed on both sides (Gerdes, et al, 1974, p. 30). Building a causeway from the mainland to Morro Rock precluded use of the north entrance after 1880, and constructing two jetties in 1942 and 1946 further stabilized the south entrance.

Morro Bay is a small estuary that traps sandy material carried into it from both the ocean and streams. The watershed for Morro Bay is only 172 km^2, and stream deposition is confined to the back bay; nonetheless, the entrance channel has to be dredged every few years. Noda and Jen (1975) concluded that most of the dredged material came from the spit, either directly from the littoral zone or from the dunes and that essentially no sand came from the back-bay streams.

Estero Bay is the site of many human activities, ranging from fishing and water-related recreation to electricity production and crude oil off-loading. A 1030 Mwt steam plant sits near the entrance to Morro Bay and the Diablo Canyon nuclear power plant resides on the south side of Point Buchon. There are five deepwater moorings north of Morro Rock for oil tankers. The oil from these tankers is pumped ashore to holding tanks and, subsequently, piped inland to refineries.

FIELD METHODS

We made detailed observations along nine transects that crossed the littoral zone from the back beach to about the 20 m contour. The northmost transect (E1) started just east of the Cayucos pier; the southmost transect (E9) started at the base of the cliffs north of Hazards Canyon. Spacing between adjacent transects was approximately 2 km. Besides surveying along the transects to establish the surface profile, we collected sand samples at several points along the transects for textural and mineralogical analysis (sample sites). At three sample sites (5 m, 12 m, and 17 m), an array of four 1-m long brass rods, driven into the sand about 70 cm, monitored local erosion or deposition (array sites). A box core was taken at each array site, and lead shot was spread on the sand surface at 10 array sites. The wavelengths of several oscillation ripples were measured at each sample site to obtain an average wavelength. Figure 2 shows the location and length of the transects, and Figure 3 shows the locations of the sample and array sites along the transects.

Profiling

For the onshore surveys, we used a device that measures distance by emitting an infra-red beam and timing its round trip to a prism. Accuracy of the unit is better than ±5 cm; inability to hold the prism rod vertical or to keep the rod from sinking into the sand became the limiting factor in such a surveying process. We also used this surveying technique across the swash and surf zones; accuracies decreased because incoming waves continually moved the rod. Surveying started at a temporary bench mark (TBM) located at the onshore end of the transect; later we tied the TBMs to nearby permanent bench marks so profiles could be plotted relative to mean sea level (MSL).

For the offshore surveys, depths were measured with a depth recorder mounted in a small boat. Horizontal positioning of the boat along the transects occurred by two methods. During the summer field season we used the infra-red surveying device because it has the capability to track a slowly moving object. During the winter field season we used a precision navigation unit, which had not been available before, because larger wave conditions precluded efficient use of the infra-red tracker. In both cases at the end of each run, the onshore surveyer noted the elevation of the boat relative to the TBM. This information permitted us to join the offshore profiles to the onshore ones without specifically knowing the tidal conditions.

Onshore surveying at a low spring tide and offshore surveying at the preceeding or following high tide provide the best chance of covering the entire littoral zone, including the area beneath the surf zone. Even so, large waves often caused a gap in the profiles between the offshore end of the beach survey and the onshore end of the boat survey.

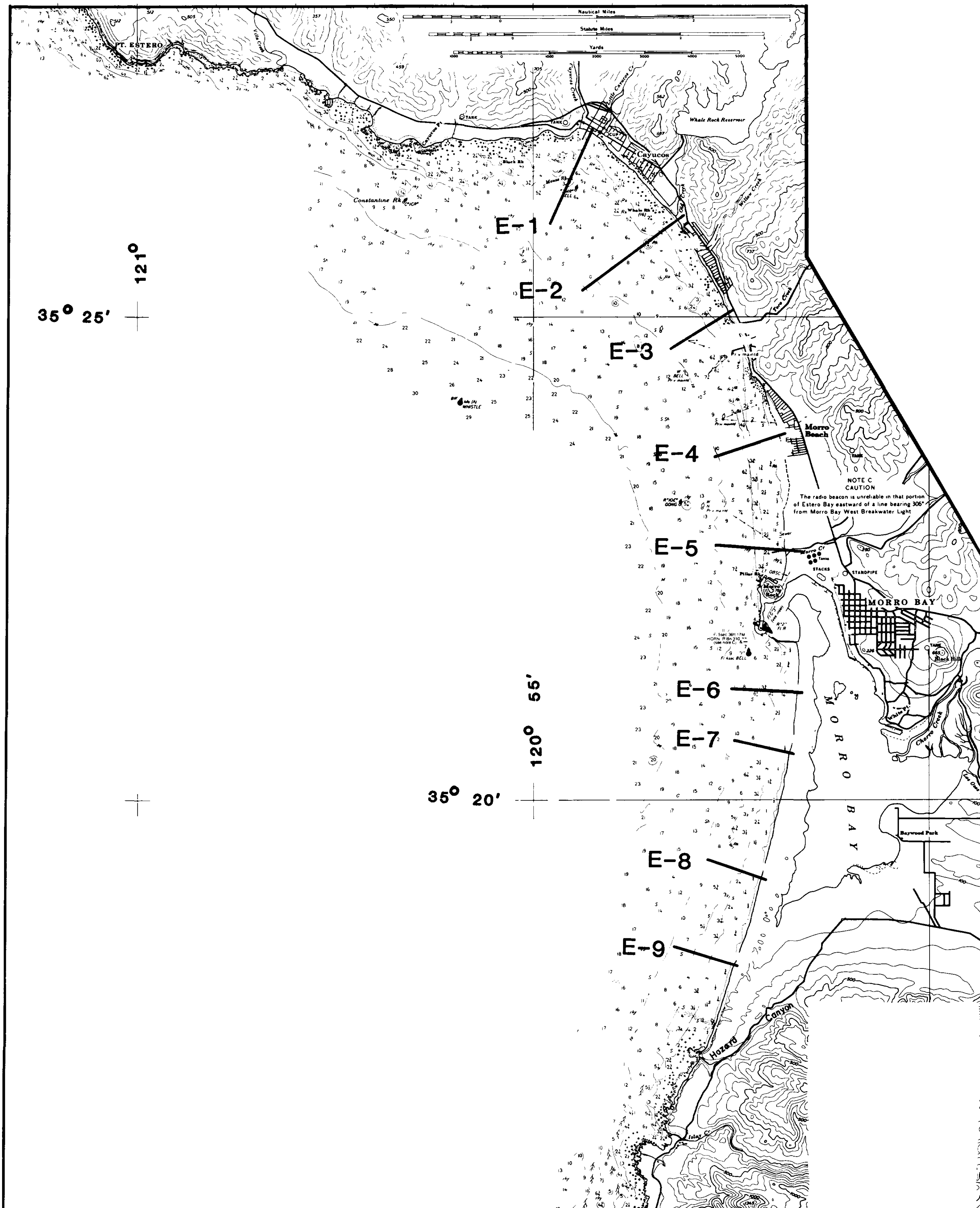

Figure 2. Locations of the nine transects within Estero Bay. Point Estero is to the west of transect E1. (Adapted from National Ocean Survey, Nautical Chart 18703, 1978).

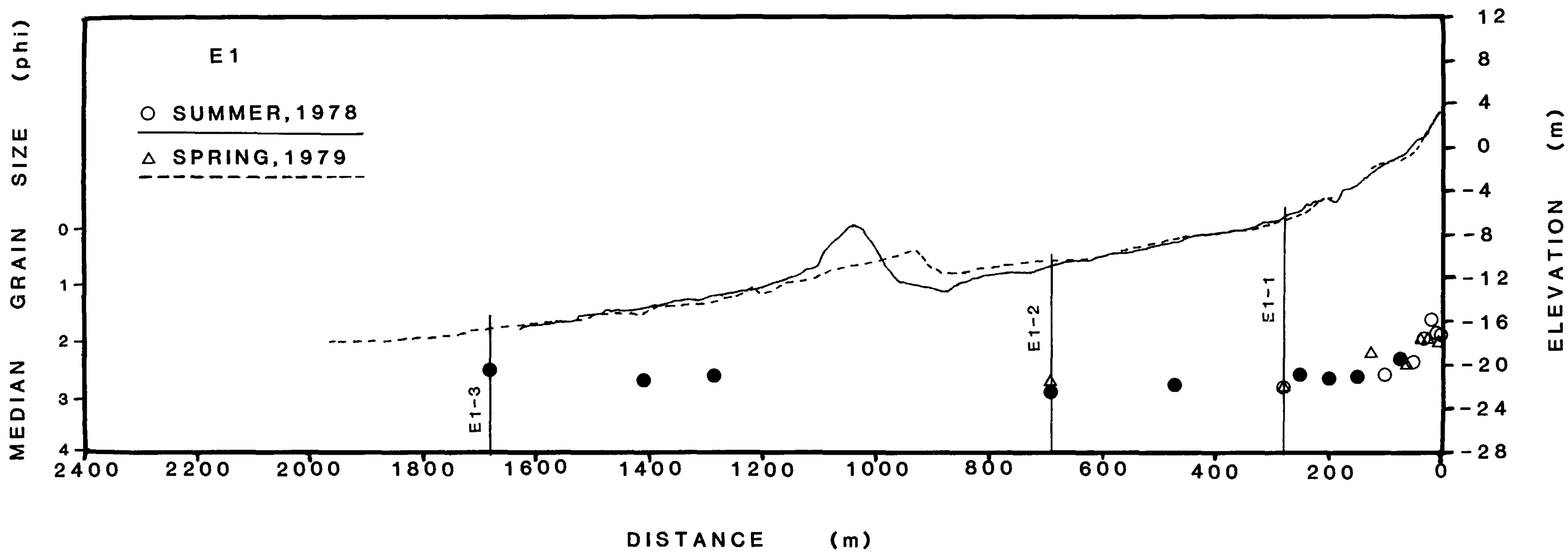

Figure 3a. Littoral-zone profiles and median grain sizes for transects E1. Mean sea level is the vertical datum. Gaps in the profiles indicate areas of no data; onshore surveys ended at the landward side of the gaps, and offshore surveys started at the seaward side of the gaps. Grain mounts were made for the solid-symbol samples. The large offshore feature is a rock; it varies in size between profiles because it is latterly variable in height, and the two surveys crossed it in slightly different places.

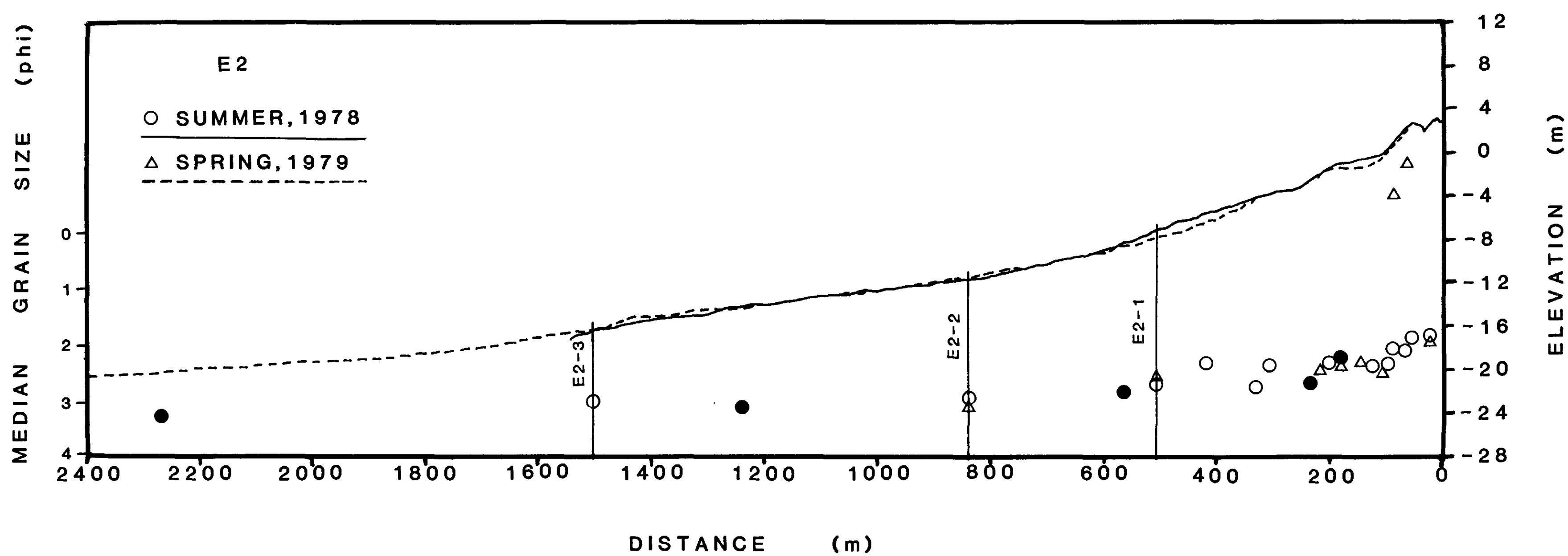

Figure 3b. Littoral-zone profiles and median grain sizes for transects E2. Mean sea level is the vertical datum. Gaps in the profiles indicate areas of no data; onshore surveys ended at the landward side of the gaps, and offshore surveys started at the seaward side of the gaps. Grain mounts were made for the solid-symbol samples.

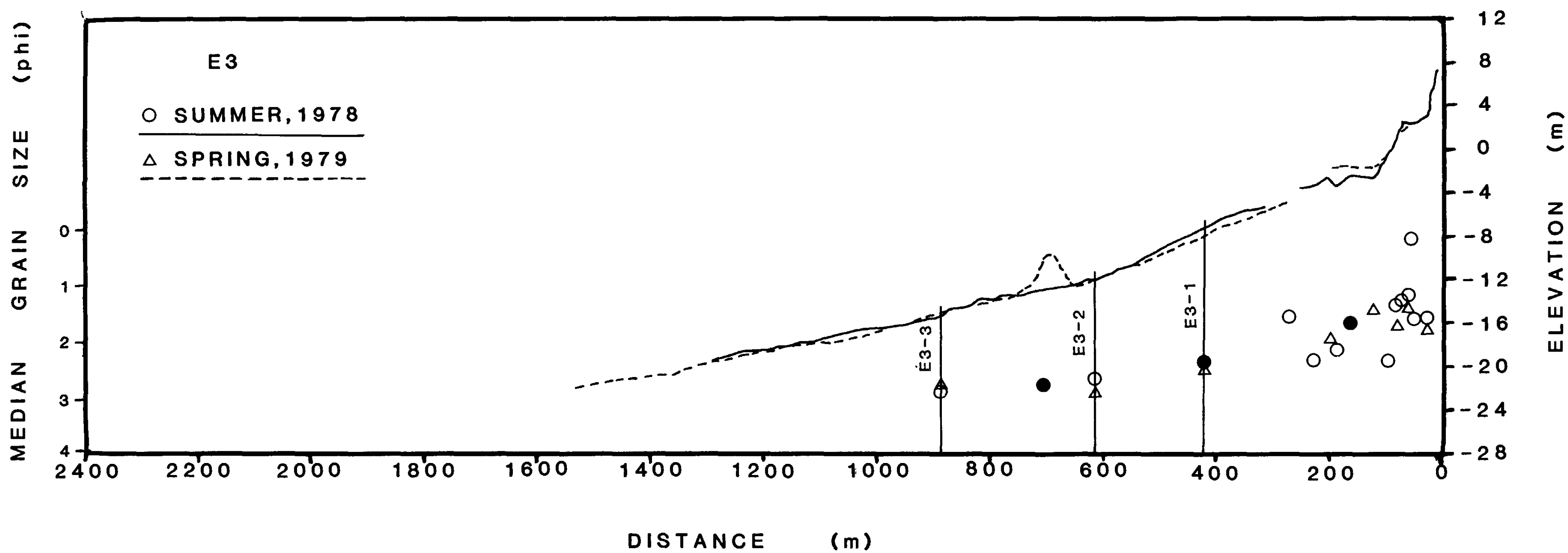

Figure 3c. Littoral-zone profiles and median grain sizes for transects E3. Mean sea level is the vertical datum. Gaps in the profiles indicate areas of no data; onshore surveys ended at the landward side of the gaps, and offshore surveys started at the seaward side of the gaps. Grain mounts were made for the solid-symbol samples. The large offshore feature is a rock; it varies in size between profiles because it is latterly variable in height, and the two surveys crossed it in slightly different places.

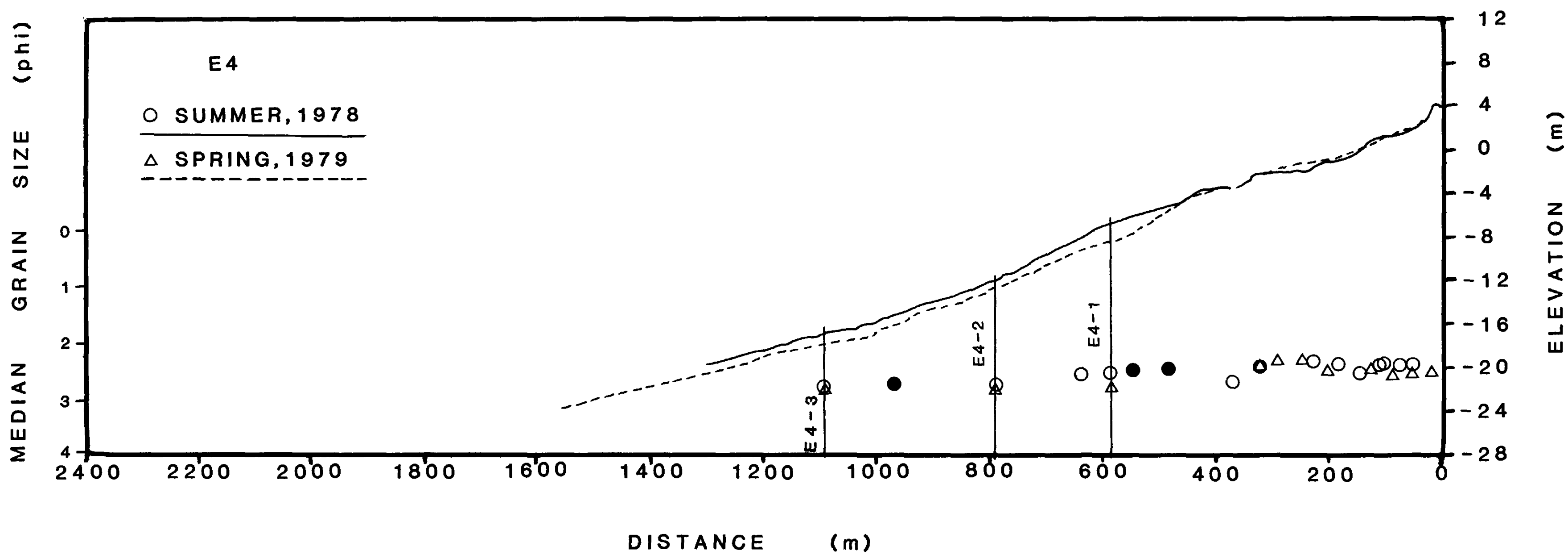

Figure 3d. Littoral-zone profiles and median grain sizes for transects E4. Mean sea level is the vertical datum. Gaps in the profiles indicate areas of no data; onshore surveys ended at the landward side of the gaps, and offshore surveys started at the seaward side of the gaps. Grain mounts were made for the solid-symbol samples.

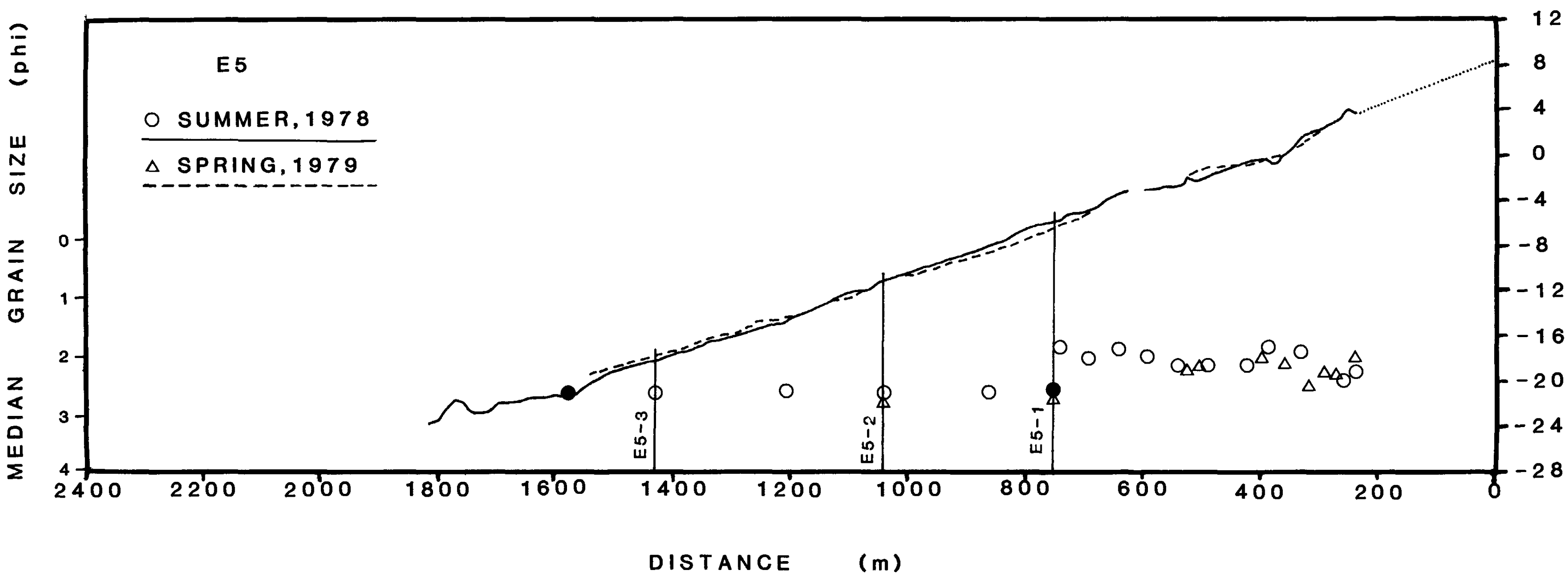

Figure 3e. Littoral-zone profiles and median grain sizes for transects E5. Mean sea level is the vertical datum. Gaps in the profiles indicate areas of no data; onshore surveys ended at the landward side of the gaps, and offshore surveys started at the seaward side of the gaps. Grain mounts were made for the solid-symbol samples.

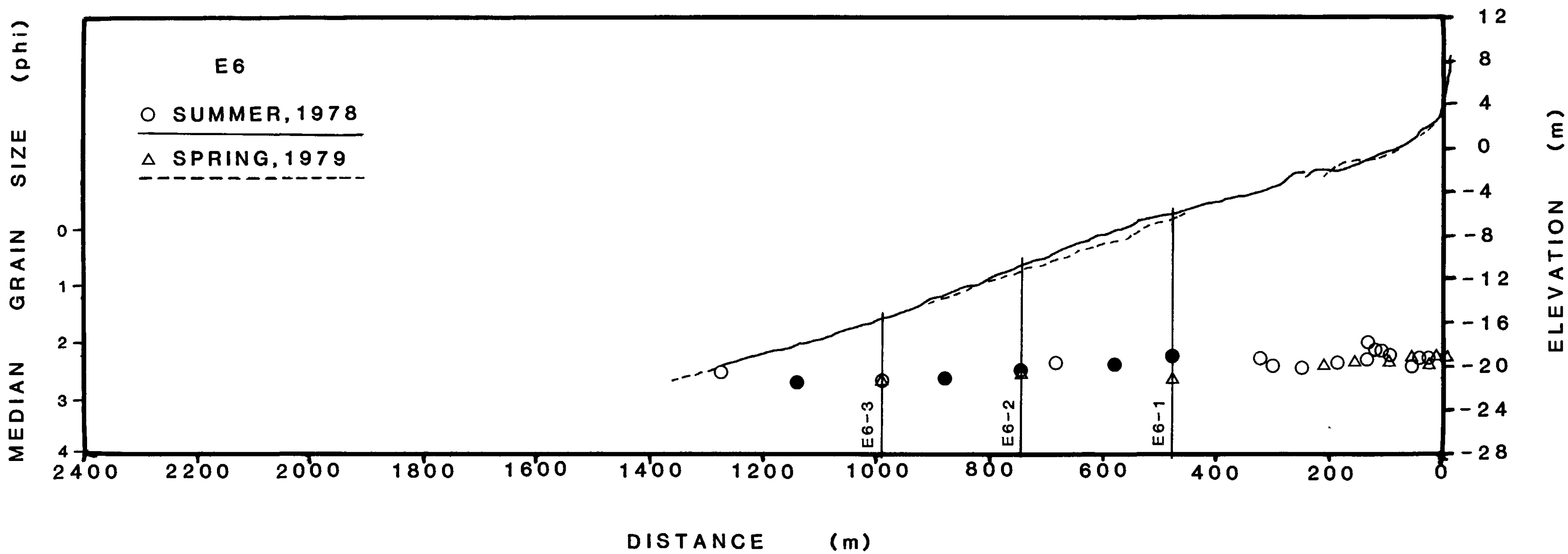

Figure 3f. Littoral-zone profiles and median grain sizes for transects E6. Mean sea level is the vertical datum. Gaps in the profiles indicate areas of no data; onshore surveys ended at the landward side of the gaps, and offshore surveys started at the seaward side of the gaps. Grain mounts were made for the solid-symbol samples.

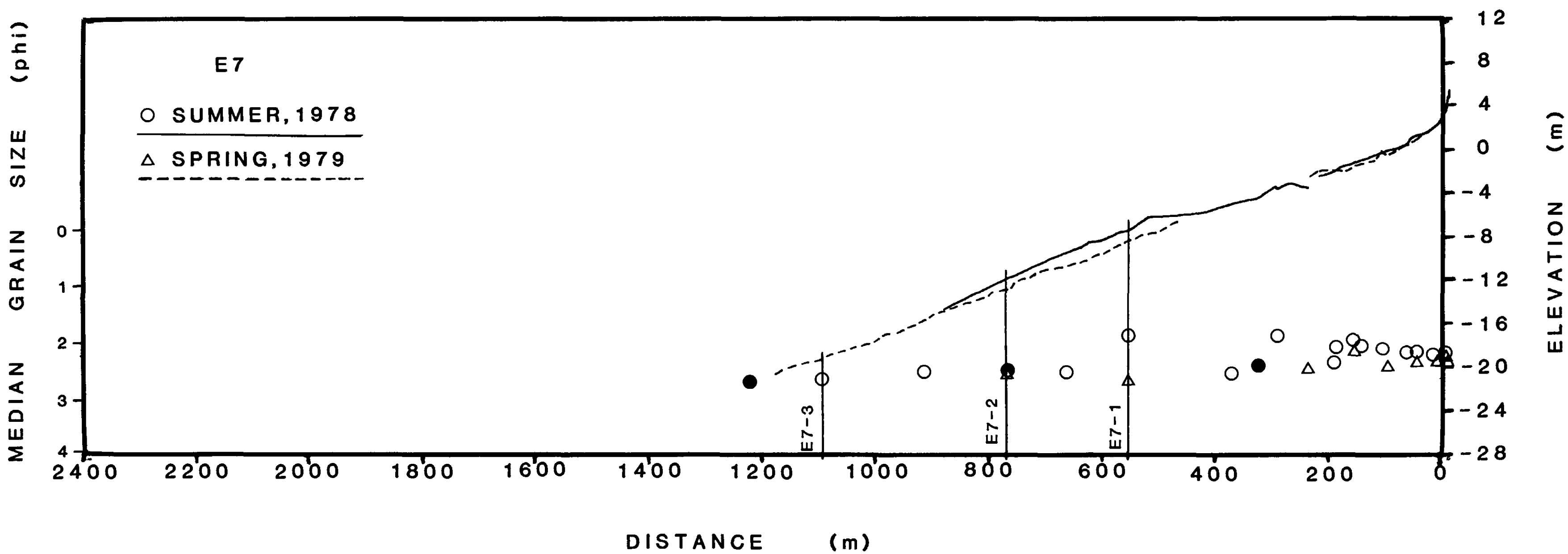

Figure 3g. Littoral-zone profiles and median grain sizes for transects E7. Mean sea level is the vertical datum. Gaps in the profiles indicate areas of no data; onshore surveys ended at the landward side of the gaps, and offshore surveys started at the seaward side of the gaps. Grain mounts were made for the solid-symbol samples.

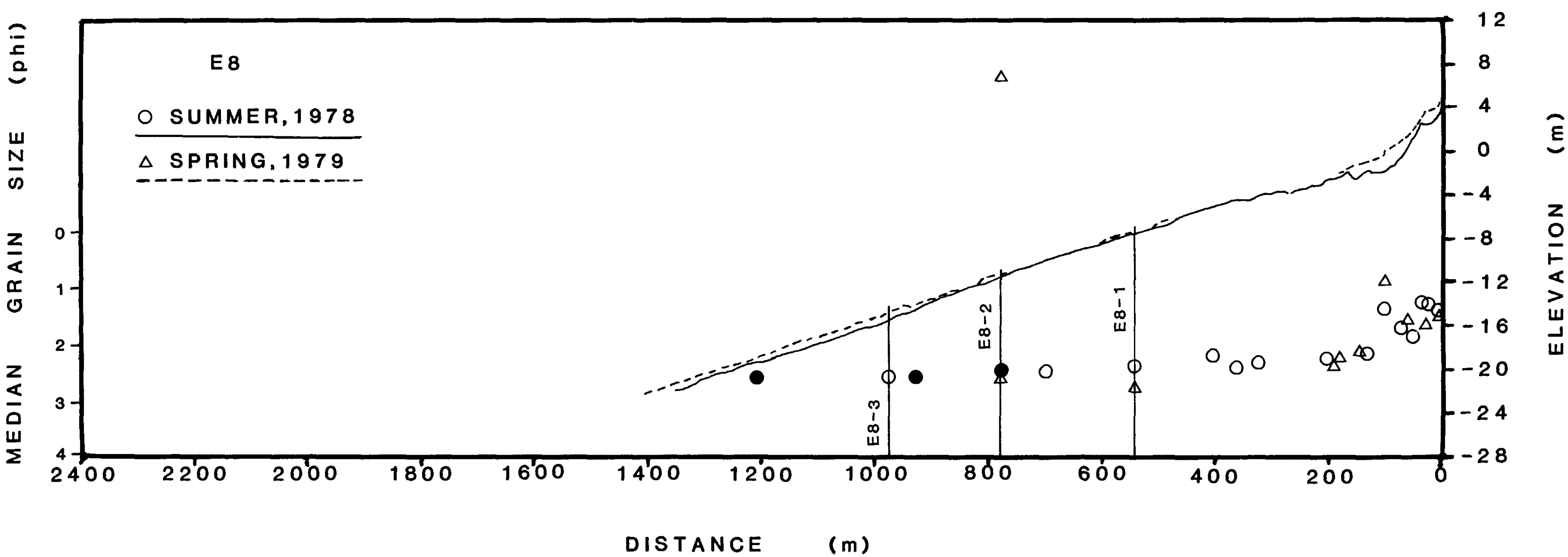

Figure 3h. Littoral-zone profiles and median grain sizes for transects E8. Mean sea level is the vertical datum. Gaps in the profiles indicate areas of no data; onshore surveys ended at the landward side of the gaps, and offshore surveys started at the seaward side of the gaps. Grain mounts were made for the solid-symbol samples.

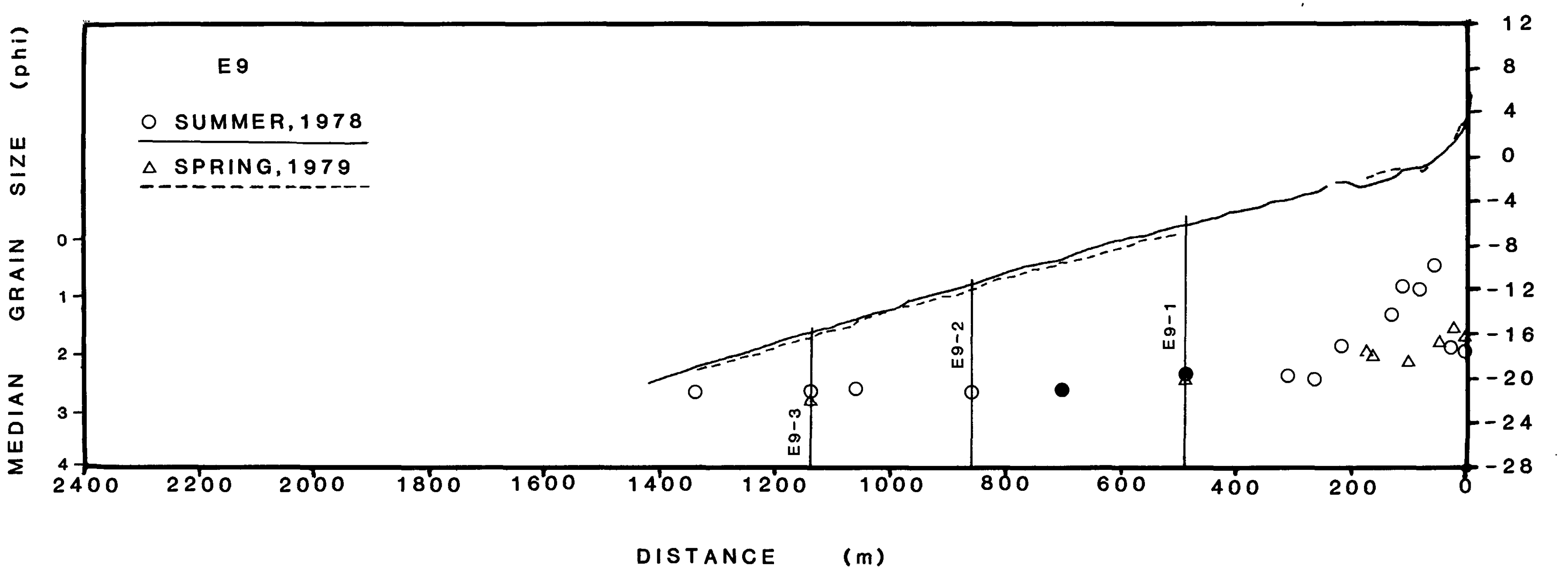

Figure 3i. Littoral-zone profiles and median grain sizes for transects E9. Mean sea level is the vertical datum. Gaps in the profiles indicate areas of no data; onshore surveys ended at the landward side of the gaps, and offshore surveys started at the seaward side of the gaps. Grain mounts were made for the solid-symbol samples.

Sand Sampling

All the sand samples came from the top few centimeters of the sediment surface. Onshore, someone scraped the sand directly into a small cloth bag; offshore, a diver collected the sample in a small plastic tube. In most instances sampling took place in conjunction with surveying, thus fixing the sample sites relative to the TBMs. Samples taken around Morro Rock, off the headlands, and along the stream beds were located from landmarks and water depth, when appropriate. Offshore, if an array could not be found, a sample was collected along the transect at the approximate depth of the array.

Surface and Internal Structures

A scuba diver recorded the ripple wavelengths by laying a clear plastic T square on top of the ripples and marking the locations of the ripple crest (Inman, 1957). Except in the transition zone very near the surf zone, wavelength is a sufficient measurement to size wave-formed ripples because ripple steepness (ratio of wave height to wavelength) maintains a constant value of about 0.16 (Dingler and Inman, 1976; Fig. 4 illustrates basic ripple parameters--wavelength λ, height η, and symmetry length β).

Boxcoring to determine internal structures followed the technique of Bouma (1964; 1969, p. 309) and resulted in a 20 cm by 15.4 cm by 8 cm core that could be epoxied and x-rayed. Cores were taken at the array sites. When taking a core, the diver oriented the corer with the longer, horizontal dimension on-offshore because this permitted better exposure of wave-formed structures. At ten of the sites, we spread a layer of lead shot on the sandy surface. The shot, which shows up in x-rays of the cores, acts as a marker because it is not readily transported away from the injection point.

A buoy, attached by polypropolene line to a 3-m pipe driven into the sand, marked each stake array except the inshore most one on line E1, which was near a fishing pier. A range served as a backup for locating the arrays if the buoys disappeared. Though ranging is subject to error because the boat often drifts off the transect, we felt that we would be able to anchor close enough to any array to find it using an underwater circle search.

Erosion/Deposition

Our technique to detect subaqueous erosion and deposition resembled the one used by Inman and Rusnak, (1956). Four brass rods were driven into the sea bottom in a T pattern with three rods located 1 m apart in a shore-parallel line, and one rod spaced 1 m shoreward of the center rod. A scuba diver scribed the location of the top of each rod onto a plastic T square that the diver stood against the rod, spanning the ripple crests. Figure 4 illustrates the array pattern and location of the coring and lead shot site.

RESULTS

The results described herein cover research carried out during most of the summer of 1978, the beginning of the spring of 1979, and a short sojourn in 1980. Because 1978 marked the start of the project, we spent almost two months reconnoitering, laying out and surveying the transects, driving in the

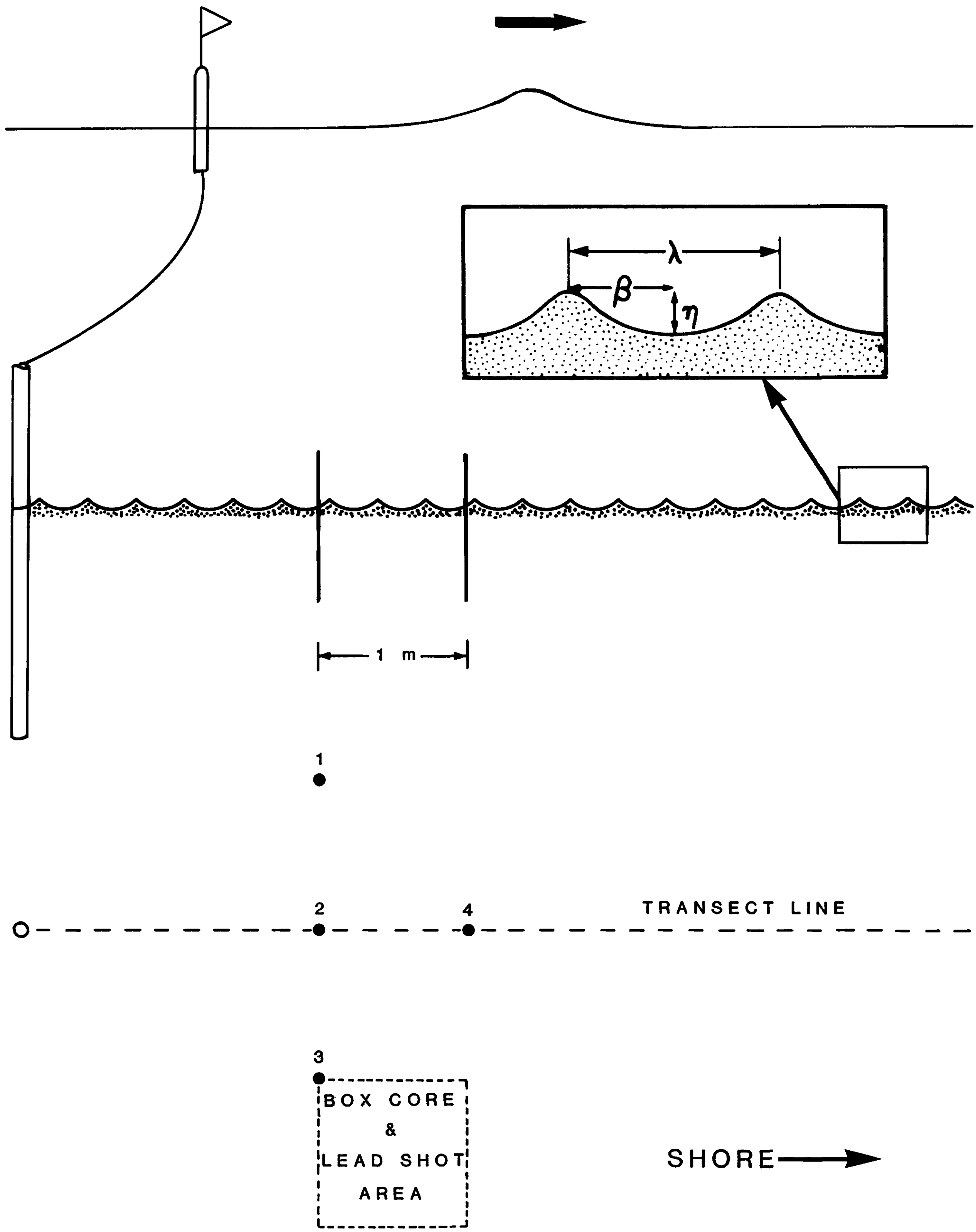

Figure 4. Diagram of the rod array layout and important ripple parameters.

brass rods and associated buoy stakes, and collecting the various underwater samples. Funding restrictions reduced the 1979 field season to two weeks and essentially curtailed subsequent field work. As a consequence, the data give a good picture of the sediment distribution within the littoral zone of Estero Bay, but are insufficient to make detailed interpretations of littoral sediment transport. Furthermore, the data show differences between summer conditions (1978 data) and winter conditions (1979 data) within the bay.

Profiles

We surveyed each of the transects in 1978 and again in 1979. The onshore and offshore parts of the 1978 surveys, which we conducted during low-to-moderate wave conditions, more-or-less overlapped on eight lines. Even so, inaccuracies in the wading technique used within the surf zone precluded resolution of any bar-like features that might have been present. Stormy conditions and time contraints during the 1979 field season prevented us from overlapping the onshore and offshore parts of any of those surveys. Therefore, surf zone features were missed completely.

We used the profile data to evaluate both temporal and spacial changes within the Estero Bay littoral zone. Figure 3 a-i compares the the 1978 and 1979 profiles. All of the plots are oriented with the beach on the right side; this is the orientation of the beach to an observer facing north. On each plot the right-most point is the location of the TBM.

Foreshore slopes ranged from 1.8 to 10.3% in 1978 (summer conditions) and from 2.3 to 8.4% in 1979 (winter conditions). During both periods the gentlest slopes occurred adjacent to Morro Rock. Offshore slopes ranged from 0.6% to 1.9% and showed essentially no change from 1978 to 1979. The gentlest slopes occurred at the north end of Estero Bay; there was very little change in slope from line E4 south. Table 1 summarizes the foreshore and offshore slope data for both 1978 and 1979.

Grain size

Textural analysis of the 169 summertime and 87 wintertime surfical sand samples turned up both areal and the seasonal patterns to the grain-size distribution within the littoral zone of Estero Bay. All of the samples were processed through a rapid sediment analyser (Thiede, 1976-1978, P. 45), and the results evaluated graphically using the technique of Inman (1952). Plots of the resulting median grain-sizes (Fig. 3 a-i; data also listed in Table 2) show that the sand in the outer part of the littoral zone is predominately fine (2 to 3 phi) with coarser sand occurring on the beach and/or in the surf zone of several lines. These plots show one trend common to most beach profiles: fining seaward along any line. They really do not clearly show another expected trend: nearshore coarsening during the winter. Offshore, the seasonal variation was negligible, although there appears to be a slight winter fining along some lines.

Heavy Minerals and Shell Fragments

Heavy-mineral grain mounts (0.62-0.125mm) were made for 36 offshore samples from the 1978 suite; 14 were point-counted in detail, and the others were given a cursory examination. Samples from Lower Cayucos Creek and Islay

Creek were also pointed-counted. The locations of the 36 samples is given on Figure 3 a-i, and the heavy mineral distributions for the 16 point counts are given in Table 3. The most common minerals in all samples are chrome spinel, epidote and clinopyroxene. Some of the grains counted as "opaque minerals" may be chrome spinel. Glaucophane occurs in every sample, but always in very low abundance. Garnet (colorless and pink) and hornblend (green and blue-green) occur in all samples in varying amounts. Orthopyroxene (enstatite or rarely hypersthene) is uncommon. Other observed minerals include sphene, apatite, zircon, tourmaline, rutile, and pumpellyite.

Generally, only very low concentrations of shell fragments appear in the samples. The exceptions to this occur at the three sites along E1. In 1980, samples taken in the rocky areas west of E1 also contained high concentrations of shell fragments, whereas samples taken in the rocky areas south of E9 had relatively few shell fragments.

Stake heights

Of the 26 buoys emplaced in 1978, 10 of 14 north of Morro Rock, but only 1 of 13 south of the rock, remained. We found two more arrays in the southern sector, but did not find the third array we searched for, which was the inshore-most array on line E7. Poor weather and high waves prevented further searches, especially in the inner parts of the southern sector.

Comparing the two sets of measurements reveals that erosion had occurred at all 13 sites (Fig. 5). At a depth of 7 m (sites E2-1, E3-1, and E4-1) erosion was extensive and increased to the south. Because we could not find array E7-1 with an underwater search even though we searched for and found the other two, more offshore, arrays on transect E7, we conclude that erosion was more extensive south of Morro Rock than north of it. At 12 m (sites E2-2, E3-2, E4-2, E5-2, and E7-2) erosion was small north of Morro Rock and extensive south of it. At 17 m (sites E1-3, E3-3, E4-3, E7-3, and E9-3) erosion was small with the same, southerly increase seen at the other depths.

Small-scale Bedforms

Oscillation ripples, undoubtedly the most widespread underwater, surficial feature in the littoral zone of Estero Bay, existed at every sample site. Although worm tubes and burrows occurred at several of the sample sites, the ripples generally showed no degradation. Crest patterns varied from short to long with the long-crested ripples generally being undulatory. At several sites shallower than 8 m, the ripple crests were discontinuous. Invariably, these sites contained a high density of sand dollars imbedded in the sand surface, which disrupted the ripple pattern.

Ripple wavelengths ranged from less than 6 cm to more than 20 cm (Table 2). Generally, we found the longest ripples in the deepest water, and the shortest in the shallowest water with an orderly transition in between. This did not occur on E1 and E2; instead, the wavelengths on these two lines oscillated back and forth along the transect. Although we visited fewer sites in 1979 than in 1978, a clear change in ripple wavelength shows up in the data. At every repeat site except two, the 1979 wavelengths were notably shorter than the 1978 ones.

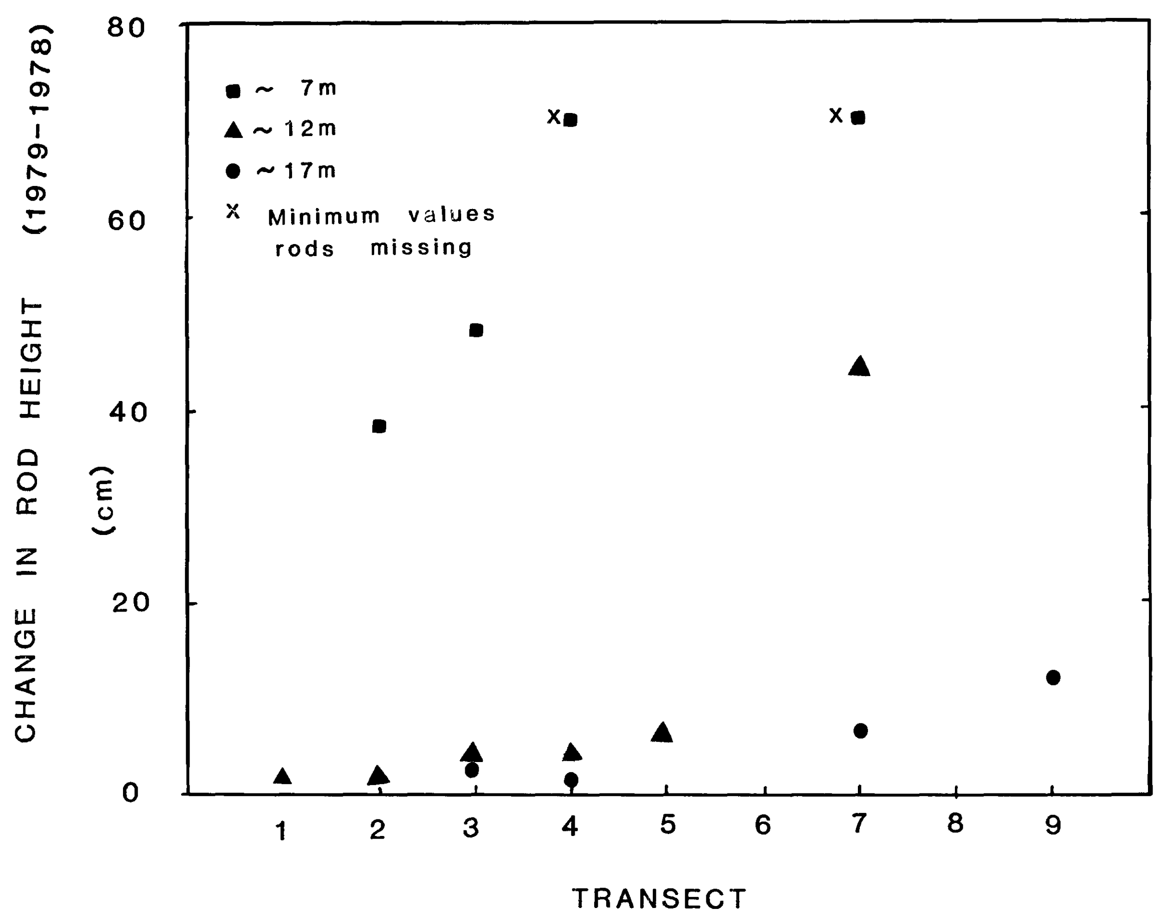

Figure 5. Plot showing the average change in rod height at the array sites that were visited both in 1978 and in 1979. Positive values indicate that net erosion occurred in the interim because the values were obtained by subtracting 1978 rod heights from 1979 heights.

Internal Structures

Anima and Dingler (1982) describe the box cores in detail; this section merely summarizes part of that data. Emphasis herein is placed on the manner in which the internal features indicate transport, erosion or depositon, or depth of wave scour.

Generally, bioturbation increased offshore, an observation made elsewhere along the California Coast by Howard and Reineck (1981). In shallower water, most of the cores predominantly show primary structures, usually as planar laminations formed by high-velocity, wave-generated bottom currents (Fig. 6). Planar lamination extends farther offshore in the 1979 cores. Crossbedding, suggestive of oscillation ripples, occurs in several of the middle and outer cores.

Although shell fragments appear to some degree in most of the cores, only core E1-3 has a high concentration. That core has a shell hash, consisting primarily of fragments less than 3 mm in greatest dimension and less than a half millimeter thick, uniformly distributed throughout it (Fig. 7). The amount of shelly material decreases rapidly both onshore and to the south.

Conversely to the trend of the shell fragments, the amount of detrital sediment that is larger than sand increases to the south, though it always appears in small concentrations. Usually this material occurs in horizontal layers that are probably lag deposits (Fig. 8).

Five sites cored in 1979 had been previously covered with lead shot in 1978; four of those cores contained lead shot (E1-3, E4-2 and-3, and E7-3). In core E4-2 only three shot appeared, and they could have been dragged down the side of the core during the coring process. The other three cores contained several shot in a horizontal layer, and in core E7-3 some of the shot appeared below the horizontal layer within a large burrow (Fig. 9). The horizontal layers of shot lay between 2.5 and 9 cm below the core surface in these cores.

Discussion

The profiles taken within Estero Bay show that offshore slopes vary systematically with the gentlest slopes being at the south end of the bay. Grain size varies systematically both alongshore and on-offshore. The mineralogical data suggest that the offshore sand is well mixed within the bay, though this conclusion is based on only a few samples. The ripple and box core data show that the littoral zone is wave dominated and that burrowing organisms are common. The stake and box core data suggest that storms cause substantial erosion in water depths at least as great as 17 m, especially south of Morro Rock.

Nearshore Zone

In an attempt to compare our beach-face data with that of Bascom (1951) and Wiegel (1964), we computed the beach slopes at mean sea level (MSL) and

Figure 6. Contact print of the x-ray of box core E2-1 (1979) showing planar bedding throughout the core. Onshore is to the right.

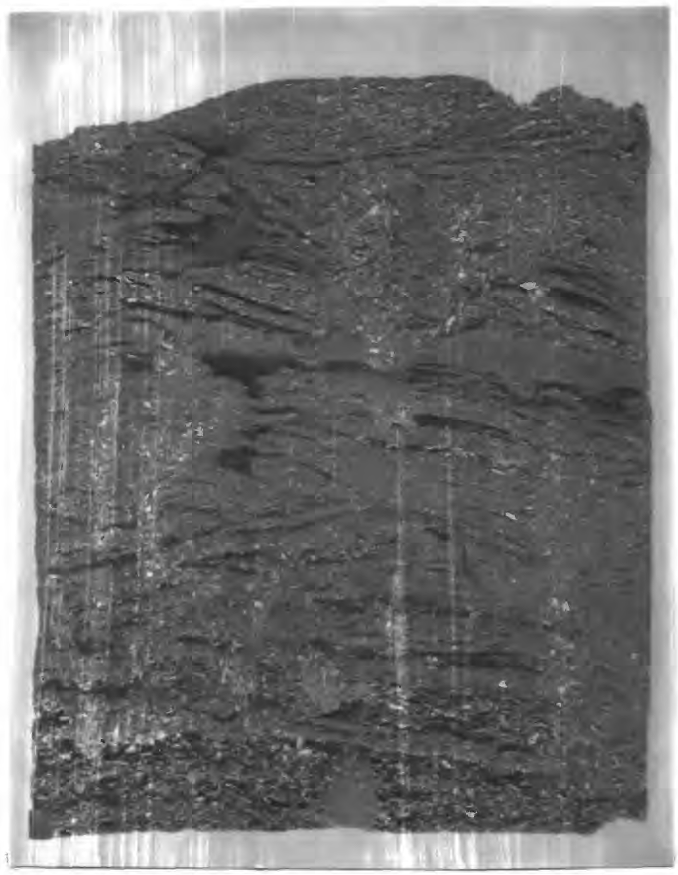

Figure 7. Photograph of box core El-3 (1978) showing high concentrations of shelly material. Onshore is to the right.

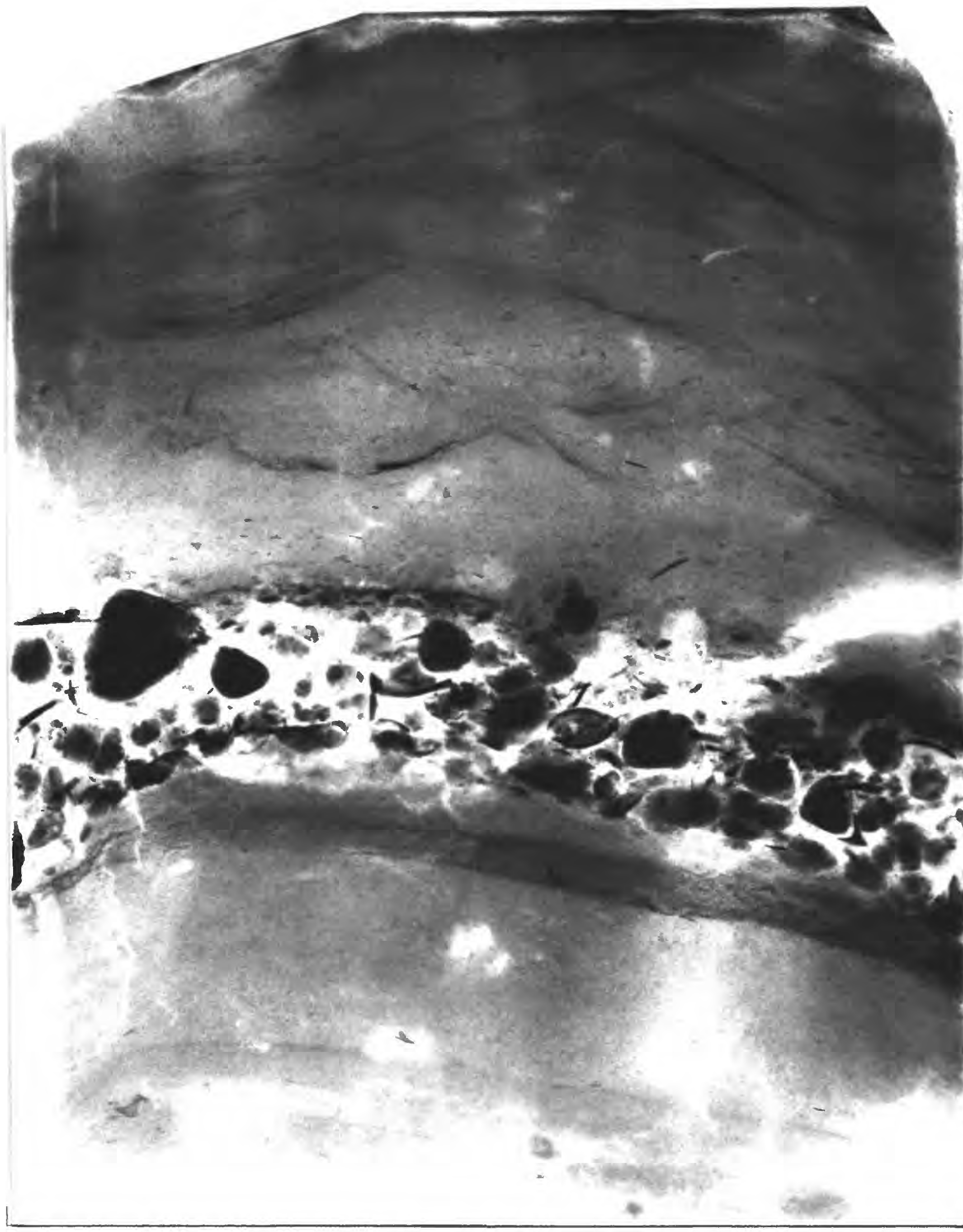

Figure 8. Contact print of the x-ray of box core E8-3 (1978) showing a gravel and shell lag deposit. Onshore is to the left.

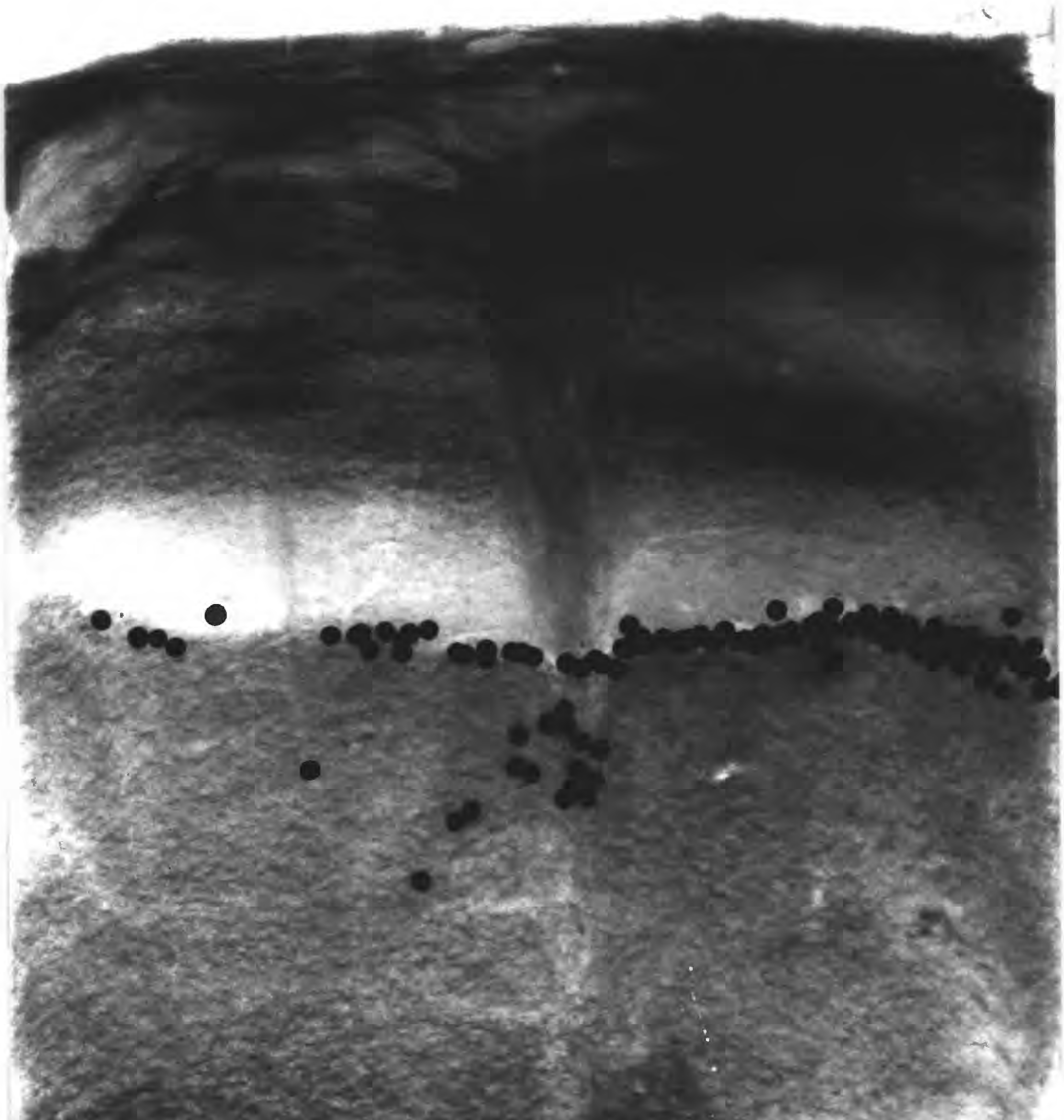

Figure 9. Contact print of the x-ray of box core E7-3 (1979) showing lead shot lying in a horizontal layer and in a burrow. Onshore is to the left.

used the median grain size of the sample at MSL. If there were no sample at MSL, we used the first one onshore. Bascom recommended that the reference point relate to the actual mid-tide elevation rather than the predicted one. We assumed that mean sea level would be the most reasonable choice for the reference point given the manner in which we sampled and profiled. In the following discussion of the beach face, slopes and grain sizes will refer to values taken at our reference point unless otherwise noted.

Foreshore slopes of Estero Bay beaches ranged from 2% to 10% in the summer and from 2% to 8% in the winter. In general, our data, which are shown in Figure 10, plot between the high- and low-energy curves drawn through the Bascom and Weigel data. Although there is scatter to the data, both summer and winter values from the northern end of the bay (E1-E4) have a strong tendency to cluster around the low-energy curve. Values from the other lines vary more, but tend to approach the high-energy curve. This over-all trend is consistent with the observation that wave energy is greater in the southern part of Estero Bay because Point Estero shields the northern part of the bay from the dominant waves. All the slopes except one are steeper than the average value given by Bascom (1951) for Estero Bay, but this is not suprising given the dynamic nature of the beach face. In fact, several measurements at each reference point are required to accurately determine the spacial variability of beaches.

South of Morro Rock, grain size and beach slope vary systematically with the coarsest material occuring at the south end of the beach in both the summer and winter. Because grain size generally decreases in the downdrift direction, this distribution suggests that the principal littoral transport direction in the south end of Estero Bay is northward.

North of Morro Rock both the largest grain size and beach slope occur in the region of E3. Grain sizes at the other four reference points are approximately equal; however, beach slope increases to the north. This trend in slope strongly reinforces the notion that Estero Bay wave energy decreases to the north.

The large grain sizes found at E3 presumably occur because of the proximity of Toro Creek, a relatively large source of sediment within the Estero Bay watershed. The smaller grain sizes at E2 and E4 relative to E3 suggest either that there is a barrier to littoral transport between E3 and the other two lines, or that the longshore component of wave energy is too small to move anything but the smallest sandy material. Outcrops bound the Toro Creek beach; however, they do not extend into the offshore and, therefore, would not greatly impede littoral transport. If Estero Bay is in equilibrium with the predominant wave energy (from the northwest), the longshore component of that wave energy would be essentially zero. Wave energy from other directions could move sediment away from Toro Creek, but this would not occur to any great degree during a year. The non-dominant waves for Estero Bay come from the southwest and, therefore, drive the sediment northward. This might explain why there is some winter coarsening on the beach face at E2, although sand carried down by spillover at the White Rock Dam could also produce the coarse fraction at E2.

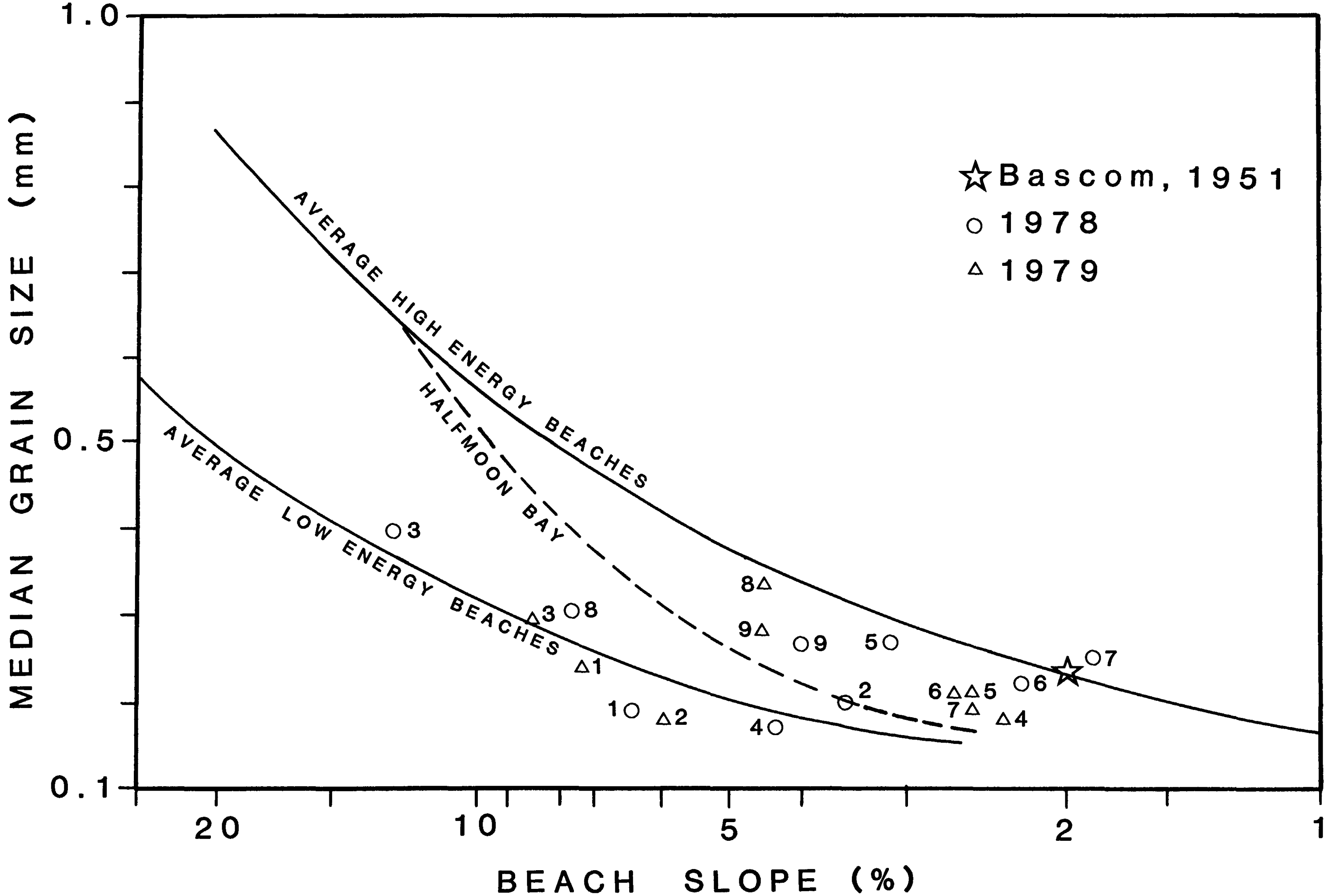

Figure 10. Plot of beach slope vs grain size that contains our data and the curves from the Bascom and Weigel data. Circles represent our 1978 data, and triangles represent our 1979 data. Numbers next to the symbols are the transect numbers. The star on the high-energy curve is the average value for Estero Bay give by Bascom (1951).

Because of the small range in grain size, it is difficult to definitively determine any trends in the data based on only two samples from each location. Two things that stand out, though, are: (1) the coarseness of the sand at E3 relative to E2 and E4; and (2) the relative coarseness of the sand occur in the summer and winter, although local variations elsewhere tend to mask them. While the cause of the difference in grain size at E3 can be explained, the cause at E8 is speculative. No streams enter Estero Bay in the vicinity of E8; in fact, the entire beach from the south jetty to the vicinity of E9 is superficially undistinguishable. Assuming the relative coarseness to be significant, the grain-size variability might be explained by either a slug of coarser material that happened to be in the vicinity during the study period, or by assuming that the area is either a high-energy focal point or a littoral transport divergence zone. Whatever the causes, the larger grain sizes at E3 and E8 exist only in the foreshore.

Offshore Zone

Offshore bottom slopes are generally the same throughout the bay except that slopes at the north end of the bay (E1 and E2) are gentler than the rest. This, coupled with the slightly smaller median grain sizes found in that area suggest that the north end of Estero Bay is a depositional zone for finer detritus. In essence, the more-or-less equilibrium shape of the bay greatly decreases the southward longshore transport that is commonly observed along the central California coast. Thus, northward transport, although small in magnitude, becomes important. Primarily, the finer material moves north and offshore until it ends up at the north end of the bay; it cannot continually follow the coastline because the east-west orientation of the coast west of Cayucos can only support easterly sediment transport. Thus, the northeast corner of Estero Bay is a convergence area. Because the primary sources of finer detritus occur north of Morro Rock, it is not possible from our data to say whether this northward migration of the finer material can also occur south of Morro Rock.

The high concentration of shell hash at site E1-3 seemingly contradicts the idea that the northern end of Estero Bay is a depositional area. Instead, it suggests low deposition, coupled with low wave energy and high productivity. The observations that the shell hash consists of small, easily destroyed fragments and that bioturbation is extensive in both the summer and winter cores from E1-3 support the idea of low wave energy in that area. A possible reason for the seemingly low deposition at E1-3 is that Mouse Rock, which is onshore of the site, acts as a barrier to the offshore movement of the finer detritus.

The mineralogical work, although not exhaustive, shows that the heavy minerals do not vary significantly with location within the bay. Because two different source-rock types with different mineral assemblages occur in the Estero Bay drainage basin--Franciscan Formation rocks to the north of Morro Rock and Monterey Formation rocks to the south--an explanation for the apparent homogeneity is that the sandy sediments have been trapped within the Estero Bay littoral cell for a long time. The lack of littoral sinks and the low sediment supply to the area promote mixing of the littoral sediment. In affect, a slow mixing of all the sandy sediments may have occurred with the only loss of sediment being to the dune field along the Morro Bay spit.

Energy Distribution and Sediment Movement

Several factors support the conclusion that a wave-energy gradient exists within Estero Bay with the highest energy to the south and the lowest to the north. Two of these factors have already been discussed: the grain-size distribution and the profile shapes in the nearshore. Other factors include: the depth of reworking of the sediment as seen in the box cores, the amount of winter erosion as evidenced by the rod measurements, and the northward increase in ripple wavelength at the offshore sites that appears to occur during the high-energy, winter months.

Considering only the rod measurements or only the box core data would result in a misleading interpretation of the subaqueous depth of scour and fill that occurred between samples; together, they give a good picture. At site E7-3, which is in 17 m of water, 11.6 cm of erosion occurred based on changes in rod height, and 8 cm of scour and fill occurred based on the location of the lead shot in the box core. This results in a maximum erosion of about 20 cm between August, 1978 and March, 1979. In comparison, the maximum erosion at E4-3 during the same period is about 16 cm (12.8 cm from the rods and 3 cm from the box core), and at E1-3 it is about 9 cm (2.1 cm from the rods and 7 cm from the box core).

At the onshore-most sites on E2, E3, E4, and E7, extensive erosion occurred between August, 1978 and March, 1979. We presume similar or greater amounts of erosion occurred at the other onshore-most sites, especially to the south, because the data from the four resampled sites show a southward increase in wave energy. By the 1979 field season no onshore sites south of Morro Bay retained their marker buoys. North of Morro Rock three sites retained their buoys (E1-1 had not been buoyed initially because of its proximity to the Cayucos pier). We assume, because we could not find site E7-1 with a circle search, that the southern buoys, whose pipes had been buried over a meter, had been removed by large waves. Of the three northern onshore most sites, the greatest erosion occurred at E4-1 (all rods missing) and the least erosion occurred at E2-1 (39 cm more rod exposed). This estimate of the depth of erosion does not include the thickness of the planar beds seen in the box cores.

Inman (1957) showed that ripple wavelength decreases with increasing near-bottom orbital diameter whenever that orbital diameter is greater than the maximum ripple wavelength for the sand in question (Fig. 11). Invariably, orbital diameter exceeds the maximum value in shallow water, open Pacific environments where the sediment is fine sand and the wave energy is high. Thus, an increase in ripple wavelength indicates lower wave energy (smaller orbital diameter); this is more-or-less the case in Estero Bay when going from south to north.

Along any 1978 transect, ripple wavelength generally decreases systematically in the onshore direction. The 1979 ripple data show a similar trend. Deviations from this trend that appear in the 1978 data may not be

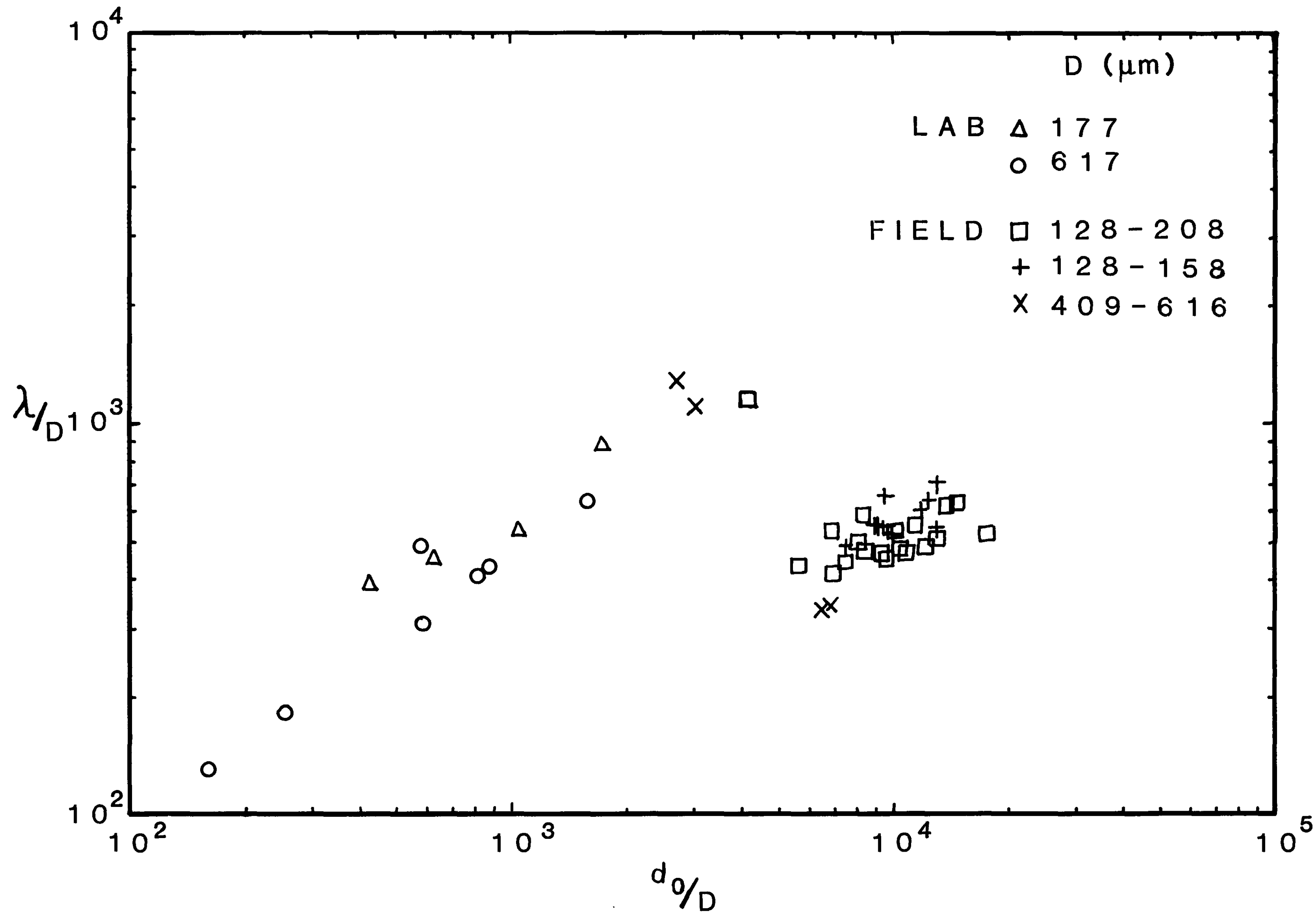

Figure 11. Orbital diameter vs ripple wavelength for various grain sizes (from Dingler, 1974).

significant, or they may occur because, during the summer, the wave energy is often not great enough to continually modify the most offshore ripples although it is high enough to modify the others. Therefore, the offshore ripples retain the characteristics of an earlier, higher energy event. Comparing specific sites between summer and winter dramatically shows the higher wave energy during the latter; the 1979 wavelengths are much shorter than their 1978 counterparts.

Littoral Cell

We did not determine the maximum depth to which on-offshore transport occurred. Both the profiles and the rod arrays show erosion during the winter. The sand could have moved into water deeper than 20 m; it could be in the surf zone, which we could not survey in 1979; or it could be on the beach and dunes.

Although our observations do not prove that Estero Bay is a littoral cell, they certainly support such an interpretation. Detailed monitoring of sediment type and movement on both sides of the two headlands would probably produce the necessary proof. If Estero Bay is a littoral cell, the offshore sands have a long residence time within the bay because sand sources seem to be small and sinks restricted to the sand dunes and Morro Bay entrance.

CONCLUSIONS

1. The shoreline of Estero Bay lies in equilibrium with the defracted and refracted waves from the northwest. This results in greatly reduced littoral sand transport to the south and, therefore, in trapping the sand within an Estero Bay littoral cell.
2. Sands are predominantly fine in size within Estero Bay. Systematic changes in grain size occur on the beach face in a longshore direction. South of Morro Rock, sand sizes decrease in a northerly direction; north of the rock they stay fairly constant except at E3, which has the coarsest foreshore material. Sand sizes decrease going offshore along every line. In the offshore, the sand remains fairly constant in size along isobaths, although there is a slight fining at the north end of the bay.
3. Beach face slopes increase to the north; offshore slopes are constant from line to line.
4. Box core and rod height data show that as much as 20 cm of scour and fill occurred in 17 m of water between August, 1978 and March, 1979. During that time more than a meter of erosion occurred in 7 m of water.
5. Oscillation-ripple wavelengths decrease in the onshore and southward directions, indicating increasng wave energy in those directions.
6. Homogeneity of the heavy minerals between widely-spaced samples suggests north and south of Morro Bay, such mixing suggests that the littoral sand moves throughout the bay and that only small amounts of sand are added to the cell.

ACKNOWLEDGMENTS

The authors thank the members of the Morro Bay Harbor Police for their help; they supplied us with laboratory and docking space and gave much useful advice about local conditions. We also thank Don Hirschaut, Charles Fletcher, Dirk Hvorka, Russel Juncal, Bruce Richmond, and Mary Lou Swisher for their help.

REFERENCES

Anima, R. J., and Dingler, J. R., 1982, Transect line location map with illustrations of box cores collected from the nearshore areas of Estero Bay, California: U. S. Geological Survey Open-File Report.

Bascom, W. H., 1951, The relationship between sand size and beach-face slope: Transactions, American Geophysical Union, v. 32, no. 6 , p. 866-874.

Bouma, A. H., 1964, Sampling and treatment of unconsolidated sediments for study on internal structures: Journal of Sedimentary Petrology, v. 34, p. 349-354.

-----, 1969, Methods for the study of sedimentary structures: John Wiley and Sons, New York, 458 p.

Bowen, A. J., and Inman, D. L., 1966, Budget of littoral sands in the vicinity of Point Arguello, California: U. S. Army, Coastal Engineering Research Center, Technical Memo no. 19, 41 p.

Bureau of Land Management, 1980, Final Environmental Impact Statement; Proposed 1981 outer continental shelf oil and gas lease sale offshore central and northern California: Department of the Interior, 2 V.

Chipping, D. H., 1979, Chorro Delta: California: Geology, v. 32, no. 3, p. 51-63.

Cooper, W. S., 1967, Coastal Dunes of California: Geological Society of America, Memoir 104, 131 p.

Dingler, J.R., 1974, Wave-formed ripples in nearshore sands: Ph.D. Thesis, Univ. of California, San Diego, 136 p.

Dingler, J. R., and D. L. Inman, 1976, Wave-formed ripples in nearshore sands: Proceedings of the 15th Coastal Engineering Conference, p. 2109-2126.

Gerdes, G. L., Primbs, E. R., and B. M. Browning, 1974, The natural resources of Morro Bay: State of California, Department of Fish and Game Report, 57 p.

Hall, C. A., 1973, Geologic map of the Morro Bay South and Port San Luis quadrangles, San Luis Obispo County, California, U. S. Geological Survey Miscellaneous Field Studies Map MF-511.

-----, 1975, San Simeon-Hosgri fault system, coastal, California: Economic and environmental implicatins: U. S. Geological Survey Open-File Report 75-533.

-----, and Pryor, S. W., 1975, Geologic map of the Cayucos-San Luis Obispo region, San Luis Obispo County, California: U. S. Geological Survey, Miscellaneous Field Studies Map MF-686.

Howard, J. D., and Reineck, H., 1981, Depositional facies of high-energy beach-to-offshore sequence: Comparison with low-energy sequence: American Association of Petroleum Geologists, v. 65, no. 5, p. 807-830.

Inman, D. L., 1952, Measures for describing the size distribution of sediments: Journal of Sedimentary Petrology, v. 22, no. 3, p. 125-145.

-----, 1957, Wave-generated ripples in nearshore sands: U. S. Army, Corps of Engineers, Beach Erosion Board, Technical Memo no. 100, 66 p.

-----, and Rusnak, G. A., 1956, Changes in sand level on the beach and shelf at La Jolla, California: U. S. Army, Corps of Engineers, Beach Erosion Board, Technical Memo no. 82, 30 p., 4 appendices.

-----, and Frautschy, J. D., 1965, Littoral processes and the development of shorelines: in Coastal Engineering, American Society of Civil Engineers, Santa Barbara Speciality Conference, p. 511-535.

Komar, P. D., 1976, Beach processes and sedimentation: Prentice-Hall, Inc., Englewood cliffs, New Jersey, 429 p.

Noda, E. K., and Jen, Y, 1975, Sand transport analysis of Morro Bay: U. S. Army, Corps of Engineers, Los Angeles District, Tetra Tech contract no. TC-467.

Shepard, F. P., and Emery, K. O., 1941, Submarine topography off the California Coast: canyons and tectonic interpretation: Geological Survey of America, Special Paper, no 31, 171 p., 4 charts.

Shepard, F. P., and Wanless, H. R., 1971, Our Changing Coastlines: McGraw-Hill, New York, 579 p.

Silvester, R., 1974, Coastal Engineering, Volume II: Sedimentation, estuaries, tides, effluents, and modeling: Elseiver Scientific Publishing Co., New York, 338 p.

Standard Oil Company of California, 1974, Draft Environmental Impact Report for Estero Bay Deepwater Terminal and Estero Bay/Richmond Pipeline Project: Standard Oil Company of California, Western Operations, Inc., San Francisco, California, 6 V.

Thiede, J., Chriss, T., Clauson, M., and Swift, S. A., 1976-1978, Settling tubes for size analysis of fine and coarse fractions of oceanic sediments: Oregon State University, School of Oceanography, Corvallis, Oregon, 87 p.

Trask, P. D., 1952, Source of beach sand at Santa Barbara, California as indicated by mineral grain studies: U. S. Army, Corps of Engineers, Beach Erosion Board, Technical Memo no. 78, 24 p.

Wiegel, R. L., 1964, Oceanographical Engineering: Prentice-Hall, Inc., Englewood Cliffs, New Jersey, 532 p.

TABLE 1

Onshore and offshore slopes and associated median grain sizes along transects lines E1 through E9. Beach-face slopes are measured at mean sea level; offshore slopes cover the most offshore 1000 m of each line. Beach-face grain sizes represent the sample taken closest to mean sea level. Offshore grain sizes represent the sample closest to 10 m below mean sea level. No 1979 offshore grain sizes are given because so few samples were collected.

LINE	BEACH FACE				OFFSHORE	
	Slope (%)		Grain size (mm)		Slope (%)	Grain Size (mm)
	1978	1979	1978	1979	1978 & 79	1978
1	6.4	7.3	0.199	0.253	0.6	0.137
2	3.5	5.8	0.207	0.188	0.7	0.146
3	10.3	8.4	0.401	0.308	1.1	0.155
4	4.3	2.3	0.178	0.187	1.5	0.171
5	3.2	2.5	0.275	0.224	1.7	0.157
6	2.2	2.6	0.230	0.215	1.7	0.182
7	1.8	2.5	0.248	0.198	1.9	0.187
8	8.0	4.3	0.308	0.342	1.7	0.165
9	4.1	4.5	0.270	0.287	1.5	0.155

Table 2. Sample-site location, median grain size, and average ripple wavelengths for the 1978 and 1979 data. Distances relate to the reference stake at the onshore end of each transect. Stars indicate that the 1979 sample was taken in the vicinity of, but not at, the 1978 array site. Two grain sizes are listed for sample E8-2 (1979); the first sample came from a patch of gravel, so a second, nearby sample was taken. The symbols X and D represent the distance from TBM and the median grain size respectively.

	1978			1979		
Sample	x(m)	D(ϕ)	λ(cm)	x(m)	D(ϕ)	λ(cm)
E1-a	4	1.85		1	2.03	
b	8	1.82		21	1.99	
c	18	1.58		35	1.98	
d	30	1.94		57	2.40	
e	49	2.33		125	2.23	
f	71	2.27				
g	100	2.56				
h	145	2.60				
i	196	2.63				
j	249	2.56				
1	279	2.78	10.2	*	2.80	
k	469	2.72	18.0			
2	687	2.87	11.5	687	2.74	15.7
l	1286	2.57	17.9			
m	1413	2.62	18.4			
3	1685	2.45	9.8			
E2-a	25	1.74		21	1.93	
b	56	1.80		65	-1.24	
c	68	2.03		87	-0.68	
d	90	2.00		107	2.46	
e	98	2.27		145	2.28	
f	126	2.31		180	2.37	
g	184	2.16		218	2.44	
h	202	2.24				
i	236	2.59				
j	307	2.29				
k	369	2.32				
l	419	2.26				
1	505	2.64	9.0	505	2.55	7.6
m	654	2.78	17.0			
2	838	2.91	12.4	838	3.10	8.7
n	1238	3.08	8.9			
3	1505	3.00	15.6			
o	2268	3.22	14.0			
E3-a	20	1.57		19	1.74	
b	43	1.54		51	1.39	
c	48	0.13		72	1.70	
d	53	1.16		94	2.29	
e	61	1.22		115	1.42	

f	72	1.32		160	1.60	
E3-g	89	2.31		190	1.94	
h	157	1.63				
i	177	2.11				
j	220	2.29				
k	264	1.53				
1	410	2.38	13.3	410	2.47	7.7
l	495	2.65	16.7			
2	605	2.69	15.3	605	2.94	9.0
m	693	2.80	11.9			
3	877	2.91	16.5	877	2.84	8.1
n	1100		15.2			
o	1300		14.8			
E4-a	48	2.34		16	2.49	
b	72	2.35		50	2.48	
c	101	2.32		84	2.51	
d	110	2.34		122	2.42	
e	141	2.49		200	2.44	
f	180	2.31		246	2.28	
g	224	2.29		290	2.28	
h	319	2.35		318	2.37	
i	368	2.62				
j	479	2.40				
k	544	2.42	10.1			
1	581	2.49	7.5	581	2.76	8.2
l	635	2.50	13.6			
2	785	2.72	17.7	785	2.81	6.6
m	967	2.70	17.0			
3	1090	2.74	19.9	1090	2.86	7.1
n	1300		14.6			
E5-a	235	2.28		235	2.03	
b	325	1.91		265	2.31	
c	385	1.86		286	2.29	
d	420	2.17		313	2.53	
e	485	2.17		353	2.16	
f	535	2.16		393	2.03	
g	585	2.04		497	2.20	
h	635	1.89		519	2.28	
i	685	2.06				
j	735	1.83				
1	745	2.57	5.7	*	2.72	
k	856	2.62	7.9			
2	1034	2.67	12.3	1034	2.80	8.2
l	1205	2.65	17.9			
3	1434	2.65	18.3			
m	1580	2.66	18.7			
E6-a	15	2.33		0	2.13	
b	38	2.16		24	2.13	
c	54	2.13		33	2.25	
d	68	2.32		67	2.19	
e	106	2.12		105	2.22	

f	121	2.03		167	2.26	
E6-g	130	2.02		220	2.33	
h	143	1.91		223	2.31	
i	197	2.29				
j	260	2.37				
k	311	2.36				
l	355	2.24				
1	487	2.21	8.0	*	2.61	
m	586	2.36	6.6			
n	694	2.33	10.7			
2	754	2.46	14.3	*	2.52	
o	877	2.61				
3	1000	2.67		*	2.69	
p	1150	2.63				
o	1300	2.58				
6						
E7-a	6	2.10		0	2.23	
b	28	2.15		6	2.14	
c	56	2.07		20	2.26	
d	78	2.10		53	2.28	
e	118	2.01		107	2.34	
g	166	1.89		220	2.18	
f	157	1.99		166	2.05	
h	170	1.87		247	2.37	
i	200	1.99				
j	201	2.26				
k	304	1.80				
l	335	2.29				
m	384	2.43				
1	565	1.82	7.8	*	2.62	
n	674	2.47	9.7			
2	779	2.42	13.1	779	2.50	7.8
o	926	2.46	17.9			
3	1104	2.59	16.1	779		8.0
p	1238	2.61	14.8			
E8-a	10	1.38		0	1.83	
b	30	1.26		10	1.47	
c	41	1.24		32	1.63	
d	55	1.85		65	1.54	
e	74	1.70		103	0.87	
f	102	1.32		148	2.11	
q	135	2.17		183	2.21	
h	206	2.21		195	2.36	
i	329	2.29				
j	369	2.38				
k	408	2.14				
1	544	2.40	6.0	*	2.74	
l	701	2.45	7.9			
2	780	2.45	10.3	*	-2.70	
					2.60	
m	927	2.56	21.0			
3	976	2.59	17.7			

n	1216	2.61	19.2			
E9-a	8	1.97		0	1.91	
b	30	1.88		6	1.71	
c	59	0.47		24	1.55	
d	86	0.91		49	1.80	
e	115	0.84		104	2.18	
f	134	1.34		165	2.06	
g	188	2.18		178	2.00	
h	269	2.47				
i	314	2.38				
1	490	2.35	10.4	*	2.45	
j	702	2.63	12.8			
2	860	2.69	19.8			
E9-k	1062	2.64	15.3			
3	1140	2.69	18.5	1140	2.83	6.9
l	1343	2.71	17.7			

Table . Heavy mineral data for selected samples from Estero Bay; all samples are from offshore except LCaC-1 and I-1, which came from the months of Little Cayucos Creek and Islay Creek respectively. Column c-o give percentages of non-opaque minerals.

SAMPLE NO.	A	B	c	d	e	f	g	h	i	j	k	l	m	n	o
E1-a	36.9	63.1	2.6	38.9	9.5	0.5	40.0	1.6	2.1	0.5	3.2	0.5	0.5	0	rutile seen
E1-3	42.5	57.5	1.7	33.9	7.9	0.4	49.6	2.1	0.4	2.1	0	0.4	1.2	0.4	
E2-6	12.2	87.8	3.0	42.3	13.6	0.4	38.1	0.4	*	*	1.5	0.4	0.4	0	
E3-2W	43.2	56.8	2.6	30.4	6.2	0.9	44.9	7.5	0.9	1.3	3.1	0.9	0.4	0.4	rutile 0.4
E4-1	17.7	82.3	4.5	36.0	13.4	*	39.3	4.5	1.2	*	0	0.4	0.4	0	chloritoid 0.4
E4-2	10.0	90.0	3.7	37.4	15.9	1.5	38.5	0.4	0.4	0	2.2	0	0	0	
E4-3	19.4	80.6	5.0	32.2	5.8	0.4	47.1	3.3	3.3	*	1.7	1.2	*	0	
E4-5	25.5	74.5	4.0	35.6	15.6	0.4	39.6	1.3	0.4	1.3	1.3	0.4	*	0	
E5-1	28.7	71.3	7.0	35.5	10.3	0.5	39.3	3.3	*	2.3	1.9	0	0	0	
E5-6	32.3	67.7	4.8	33.8	12.9	0.5	40.0	7.1	0.5	0.5	0	0	*	0	
E6-2	16.7	83.3	2.4	35.4	19.3	*	39.0	1.6	0.4	*	2.0	*	*	0	
E7-3	18.6	81.4	2.8	35.4	11.2	0.7	44.2	3.2	0.4	*	1.8	0	0.4	0	
E8-m	33.1	66.9	4.4	23.1	11.6	*	52.6	6.8	0	0.4	0	*	0.8	0	rutile 0.4; staurolite seen
E9-1	32.9	67.1	2.4	33.3	16.1	1.2	40.8	4.3	0	0.4	0.4	0.8	*	0	
LCaC-1	34.4	65.6	2.0	31.0	5.6	1.0	48.7	5.1	1.5	4.1	0.5	0	0.5	0	
I-1	60.6	39.4	3.4	29.4	9.2	0.8	37.8	11.8	0.8	4.2	0	0	0.8	0.8	rutile 0.8

*Mineral seen but not encountered in point-count

A-Opaque Minerals - includes chrome spinel.
B-Non-opaque Minerals
c-Orthopyroxene
d-Clinopyroxene
e-Hornblende - mostly green, with small, approximately equal amounts of blue-green and brown.
f-Glaucophane - grains sometimes show epidote attachment.
g-Epidote - includes clinozoisite and non-Felzoisite.
h-Garnet - colorless, pale and deep pink, rarely pale to deep yellow.
i-Sphene
j-Zircon - commonly colorless; a few pink grans are present.
k-Pumpellyite
l-Tourmaline - blue and brown; some grains show both colors.
m-Apatite
n-Unknowns
o-Others